Alpine high pressure evolution of the eastern Bitlis complex, SE Turkey

R. OBERHÄNSLI[1]*, O. CANDAN[2], R. BOUSQUET[1], G. RIMMELE[1], A. OKAY[3] & J. GOFF[4]

[1]*Institute of Geosciences, Potsdam University, Karl Liebknecht Strasse 24, 14476 Potsdam, Germany*

[2]*Institute of Geosciences, Dokuz Eylül Üniversitesi, Mühendislik Fakültesi, Tınaztepe Yerleşkesi 35160 Buca/İzmir*

[3]*Schlumberger, Well Service, Clamart, France*

[4]*Istanbul Technical University, Eurasia Institute of Earth Sciences, Maslak 34469 Istanbul Turkey*

Q1 [5]*BP Exploration Operating Co. Ltd, Middlesex, UK*

**Corresponding author (e-mail: roob@geo.uni-potsdam.de)*

Abstract: The Bitlis complex, SE Anatolia, constitutes a crystalline complex derived from the north of the Arabian Plate, accreted to the South Armenian block. Metamorphic studies in the cover sequences of the Bitlis complex allow constraining the thermal evolution of the massif by metamorphic index minerals. A regionally distributed low temperature-high pressure (LT-HP) metamorphic evolution is documented by glaucophane, relics of carpholite in chloritoid-bearing schists and pseudomorphs after aragonite in marbles. The metamorphic age of these HP assemblages is constrained by Ar isotope dating as 74 ± 2 Ma. This indicates that (i) the Bitlis complex represents a terrane detached from the Arabian indenter that was subducted and stacked to form a nappe complex during the closure of the Neo-Tethys and (ii) that during Late Cretaceous to Cenozoic evolution the Bitlis complex never underwent temperatures over 450 °C. The consequences of the metamorphic evolution of the Bitlis complex – a cold continental block within a hot environment- for the Eastern Anatolian plateau are complied in a crustal section.

The Bitlis complex is situated at the front of the Eurasian plate collage overriding the Arabian platform. This mountain belt, pinched between the Taurids and Zagros (east–west) as well as Caucasus and Arabian plate (north–south), is part of the southern edge of a high plateau that extends northward to the Caucasus. Recent investigations in southern Armenia revealed blueschists along the Sevan Akera suture zone, the metamorphic age of this high-pressure (HP) metamorphism event is 95 to 90 Ma (Rolland *et al.* 2008). Recent seismologic work revealed normal crustal thickness (*c.* 40 km) and a reduction in seismic velocities at depth (Zor *et al.* 2003; Gök *et al.* 2007). This is interpreted as asthenospheric upwelling and a missing of the lithospheric mantle lid (Sengör *et al.* 2003; Lei & Zhao 2007). Geophysics showed that this is a critical area for the geodynamic evolution as well as the dynamics of the North Anatolian fault system (Facenna *et al.* 2006). All geodynamic models, mostly supported by geochemical investigations of volcanic rocks (Keskin 2003) presented so far (Sengör *et al.* 2003; Keskin 2003; Lei & Zhao 2007) assume that the Bitlis-Püturge complex was situated in an arc position. As far as geological information is considered, some of the early reports of the geological survey (MTA) are difficult to access for international readers. Göncüoglu and co-workers mapped part of the Bitlis metamorphic complex, between Bitlis and Mus, during the 1980s. Parts of this work were published as a short compilation (Göncüoglu & Turhan 1984).

We present new investigations on the metamorphic petrology of the Bitlis complex, gathered in the context of the Middle East Basins Evolution programme (MEBE). The aim of this study is to understand the Alpine geodynamics of the eastern Bitlis complex by adding knowledge to the structural and thermal evolution. The consequences of these new findings for the geodynamic evolution of Eastern Anatolia and the high plateau that built up between the Arabian and the Eurasian plates are discussed. In this paper we report occurrence and age of HP metamorphism indicative minerals

From: Stephenson, R. A., Kaymakci, N., Sosson, M., Starostenko, V. & Bergerat, F. (eds) *Sedimentary Basin Tectonics from the Black Sea and Caucasus to the Arabian Platform.* Geological Society, London, Special Publications, **340**, 461–483. DOI: 10.1144/SP340.20 0305-8719/10/$15.00

in meta-sediments and mafic metamorphic rocks from the Palaeozoic to Mesozoic cover of the Bitlis complex.

Geological setting of SE Turkey

The Bitlis complex forms an arcuate metamorphic belt, about 30 km wide and 500 km long, rimming the Arabian Platform in SE Anatolia (Fig. 1). It is separated from the Arabian Platform by a narrow belt of Upper Cretaceous to Eocene flysch and ophiolitic mélange and Miocene sediments. Along the Northern front of the Arabian indenter a set of collisional autochthonous and allochthonous massifs is known. From south to north, these are: the Great Zap anticlinorium; the Eocene olistostrome of the Hakkari complex overlain by Cretaceous mélanges of the Yüksekova complex; the metamorphics of the Bitlis complex; and finally the Quaternary volcanics north of Lake Van. The Bitlis metamorphic complex comprises Precambrian to Cretaceous rocks and builds up the uppermost tectonic unit of the area. It is covered by Cenozoic sediments and Quaternary volcanics in the north and overlies Cretaceous (Yüksekova complex) and Eocene to Miocene series, the Hakkari and Maden complexes (Baykan and Ziyaret Formations, south of Bitlis), as well as the sediments of the northern margin of the Arabian autochthon. In an early description, Tolun (1953) interpreted the metamorphic rocks of the Bitlis complex as forming the basement of the region. According to Kellogg (1960) and Göncüoglu & Turhan (1984) the Bitlis metamorphics are equivalents of the Arabian autochthonous succession and are assigned a Devonian–Upper Cretaceous depositional age to the meta-sediments. First detailed descriptions of the Bitlis complex were given by Boray (1975), Cailavan *et al.* (1984), Yilmaz, (1978) and Hall (1976). Horstink (1971), Sungurlu (1974) and Sengör & Yilmaz (1981) proposed various geodynamic interpretations. In their paper Göncüoglu & Turhan (1984) suggested that the basic geological data used in earlier interpretations were remarkably incomplete. A remark that still holds true for these eastern areas! The legend of Figure 1 adapts the formation names after Perincek (pers. comm. MEBE). For our compilation we used older literature and different formation names.

Lithostratigraphy and metamorphism of the Palaeozoic to Mesozoic Bitlis complex

In the following paragraphs we present a synthesis of the geology of the Bitlis complex mainly based on Turkish literature. A generalized lithostratigraphic section is comprised as follows from bottom to top.

- The pre- to infra-Cambrian Hizan group, composed of gneisses, meta-basic rocks and schists separated into three formations: the Andok augengneiss with biotite, muscovite, amphibole, the Ünaldi Formation with amphibolites and garnet-amphibolites with relics of eclogite (Okay *et al.* 1985) and the Ohin schists containing biotite, muscovite, garnet and amphibole.
- Palaeozoic rocks of the Mutki group unconformably overlie the Hizan group. The base of this rock group is made of the Devonian Meydan Formation comprising meta-conglomerates, quartzites and greenschists with limestone interlayers, reef limestones and albite-chlorite-actinolite-chloritoid schist's of probably volcanogenic origin. The Meydan Formation grades into the volcanoclastic Çesme Formation consisting of felsic meta-volcanic and meta-tuffs. Both formations are intruded by the Mus meta-granite and the Çesme Formation is considered to be the product of this magmatism. The age of the felsic meta-volcanic rocks is reported as *c*. 454 Ma based on Rb–Sr whole rock analyses (Yilmaz *et al.* 1981) The leucocratic granitoids have wide exposures north of Hizan, north of Mutki and southwest of Mus. Their age is badly constrained (Helvaci & Griffin 1984). They are not affected by the Precambrian regional metamorphism but feldspathized meta-volcanic rocks reveal an age of *c*. 91 Ma while from the Avnik granite an amphibole-whole-rock-feldspar age of 71 Ma, a biotite-whole-rock age of 41 Ma and from micaschist a chlorite-muscovite age of 38 Ma are reported (Helvaci & Griffin 1984). These late Alpine mineral ages are interpreted to reflect recrystallization during emplacement deformation. Rb–Sr and K–Ar white mica ages from the Mus granite are Late Cretaceous (73–107 Ma) (Göncüoglu 1984).
- All three units, Meydan Formation, Çesme fm, and Mus meta-granite are unconformably overlain by the Çirrik Limestone, which is a sequence of recrystallized limestone inter-bedded with chloritoid schists and graphite schists. This sequence grades up into calcschists and thin-bedded recrystallized limestones. A Lower Permian age is assigned to these rocks. On top of these thinly bedded meta-carbonates a sequence of coarsely bedded recrystallized limestones with interlayers of calcschists, meta-sandstones and chlorite schists of Upper Permian age, the so-called Malato Formation, was deposited.

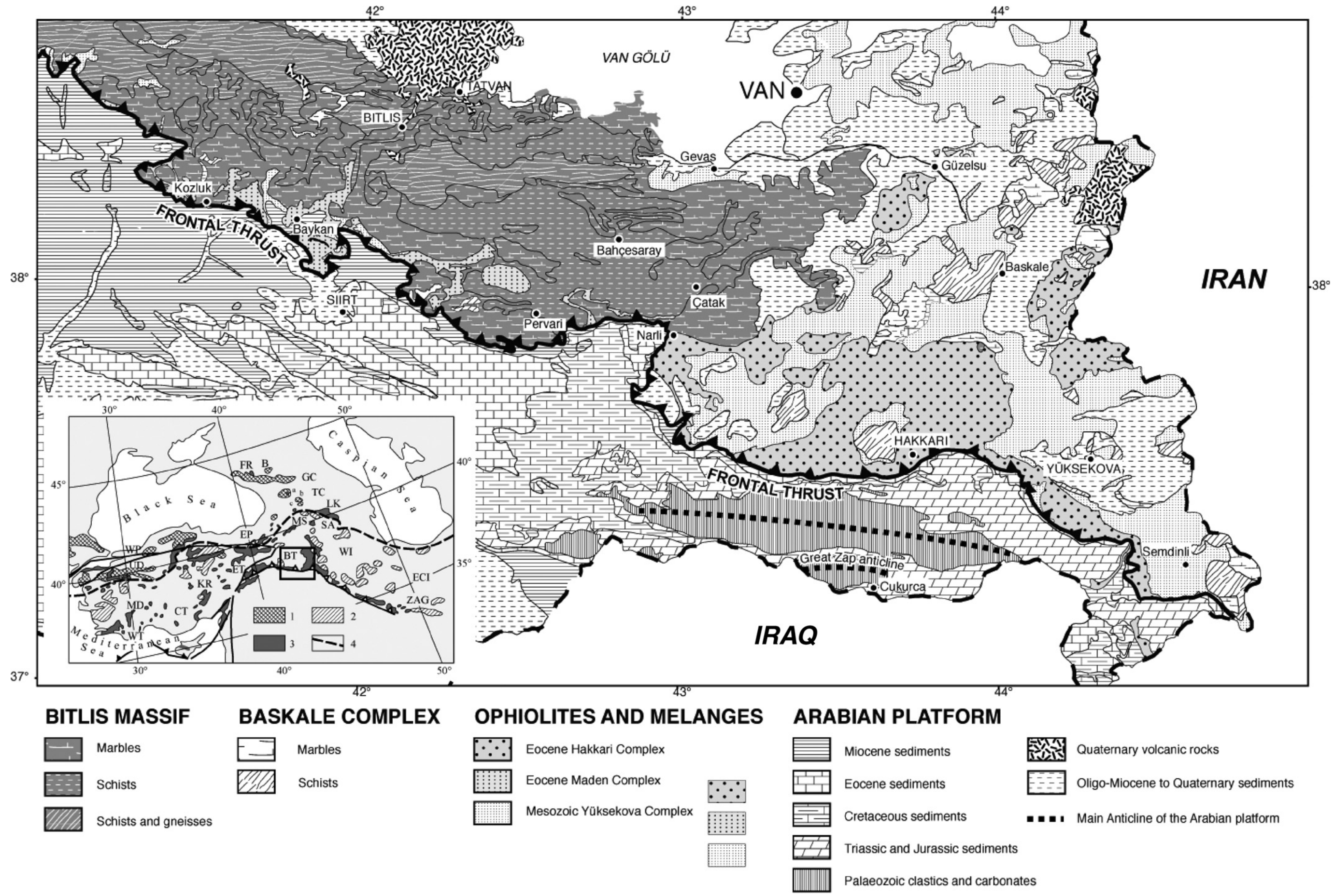

Fig. 1. Geological map of the Eastern Bitlis complex (modified after MTA 1:5 000 000 maps Cicre and Van). Inset: Sketch of ophiolite zones and crystalline basement salients of the Eastern Mediterranean Province. 1, salients of the Hercynian granite-metamorphic basement; 2, salients of the Precambrian granite-metamorphic basement; 3, ophiolite complexes and zones of serpentinite mélange; 4, inferred suture of Palaeozoic Tethys. Abbreviations: WP, EP, Western and Eastern Pontides; WT, CT, ET, Western, Central and Eastern Taurides; MD, Menderes massif; KR, Kirshehir massif; UD, Ulu Dag massif; BT, Bitlis complex; FR, Fore Range zone of the Great Caucasus; B, Bechasine zone; GC, Main Range of the Great Caucasus; TC, Transcaucasian massif (a, Dzirula; b, Khrami; c, Lokhi and Murguz salients); LK, Lokhi-Karabakh zone; SA,Sevano-Akera zone; MS, Miskhan massif; WI, ECI, Western Iran and Eastern Central Iran; ZAG, Zagros; A, Alborz. Boxed area is the region of study.

- The Triassic rocks of the Tütü Formation form the upper part of the Mutki group, the base of which consists of recrystallized limestones and calcschists grading upward into meta-shales, met tuffs, meta-diabases and meta-basalts and finally meta-conglomerates, meta-mudstones and shales, indicating a drastic change in depositional conditions. The upper part of the Mutki group contains meta-quartzporphyres. They are interpreted as being the result of the opening of the Tethys Ocean.

The Bitlis complex has undergone a low to medium-grade Alpine metamorphism (Sengün 1993). K–Ar ages from the western part of the Bitlis complex near Pütürge gave 71.2 $\pm$ 3.6 Ma (Hempton 1985). Helvaçi & Griffin (1984) reported similar mineral ages from the Bingöl area in the western part of the Bitlis complex.

The Mesozoic ophiolitic sequences

Tectonically underlying the Tütü Formation ophiolitic mélanges are found. They have been termed the Güleman ophiolites (Göncüoglu & Turhan 1984) after the Upper Jurassic–Lower Cretaceous sequence found far to the SW of the Bitlis region. Eastward in the Van and Hakkari regions, the term Yüksekova complex is used because it is more of an ophiolitic mélange than a regular ophiolite. In the ophiolitic mélanges near Mutki glaucophane-bearing blocks have been described (Hall & Mason 1972). In the Hakkari-Narlı region it forms large flat-lying klippen over the Eocene-aged Hakkari complex, and is tectonically overlain by the Bitlis metamorphic rocks. In the Bitlis-Baykan, region it forms tectonic slivers between the Bitlis metamorphic rocks and the underlying Maden complex. The Yüksekova complex has a mélange-like internal structure and represents a strongly deformed accretionary complex. It consists of a chaotic jumble of basalt, gabbro, serpentinite, pelagic limestone, radiolarian chert, neritic limestone, granodiorite, sandstone, siltstone, and shale with an estimated vertical thickness of about 2000 metres. The youngest limestone blocks found in the Yüksekova complex give Coniacian–Campanian ages (Perinçek 1990). SE of the mélange complex in the Cilo mountains the Oramar and Karadas ophiolites are reported (Özkaya 1982). Ophiolitic rocks also crop out north of the Bitlis complex on the shores of Lake Van. This Gevas 'ophiolite' is of special importance as it lays directly under the Bitlis metamorphic rocks (Yılmaz *et al.* 1981), implying large-scale allochthony for the Bitlis complex. The Gevas 'ophiolite' is a disordered ophiolite consisting of serpentinite, gabbro, basalt and limestone blocks. Some of the limestone blocks have yielded Maastrichtian rudists (Özer 1992) showing an Arabian rather than a Taurid affinity.

Lithostratigraphy of Cenozoic complexes

From the western parts of the Bitlis complex, mélanges discontinuously overlie non-metamorphic wildflysch and olistostromal units of the Upper Maastrichtian (Kinzu Formation and Kizilgic Formation after Göncüoglu & Turhan 1984). The upper contacts of these Eocene formations have been described as tectonic. This indicates that the Bitlis complex acquired its structure after the Late Eocene times.

In the area of investigation, a belt of two complex assemblages occurs below the Bitlis complex and the ophiolitic mélanges: the Hakkari complex and the Maden complex.

The Hakkari complex covers large areas southeast of the Bitlis complex, between Narlı and Yüksekova, where it tectonically overlies the Eocene and Miocene formations of the autochthon. It is equivalent in time to the Maden complex, which crops out widely farther west. The Hakkari complex differs from the Maden complex by the scarcity of the volcanic rocks. The Hakkari complex is divided into two formations, a lower unit called Urse Formation and an upper mélange-type unit named as the Durankaya complex (Perinçek 1979, 1990; Yılmaz & Duran 1997). The Urse Formation consists predominantly of slightly metamorphosed siltstone, shale and fine-grained sandstone with limestone intercalations. It is well exposed on the Baskale-Hakkari road, where it starts with fine-grained metabasites and passes into a very thick slate series. Near Hakkari, the slates are overlain by medium-bedded dark carbonates.

The Durankaya complex tectonically overlies the Urse Formation and consists of blocks of pelagic and neritic limestone, serpentinite, gabbro, basalt and amphibolite in a strongly deformed shale matrix. Some of the pelagic limestone 'blocks' probably represent original limestone intercalations. Such limestones have yielded pelagic and neritic foraminifera of Early to Mid-Eocene age (Perinçek 1990; Yılmaz & Duran 1997).

The Maden complex is of the same age as the Hakkari complex in regions west of Narlı. It differs from the Hakkari complex by the presence of abundant volcanic rocks. It widely crops out along the southern margin of the Bitlis complex, as tectonic slivers either directly under the Bitlis metamorphic rocks or through an intervening thrust sheet of the ophiolitic mélange (Yüksekova complex). The Maden complex consists of sandstone, conglomerate, red pelagic limestone, basaltic lava, and tuff. Limestones in the Maden complex yield Lower to Middle Eocene foraminifera. In a few localities the Maden complex is reported as lying unconformably over the Bitlis metamorphic rocks. However, in most places it is positioned between the Cenozoic formations of the Arabian Platform and the Bitlis complex. Yigitbas & Yılmaz (1996) regard the Maden complex as products of a short-lived Mid-Eocene back-arc basin, above the northward-dipping subduction zone between the Arabian Platform and the Anatolide-Tauride Block as represented by the Bitlis complex. Around Baykan, south of Bitlis, the Maden complex (locally named as the Baykan complex by Göncüoglu & Turhan 1992) is lithologically highly variable. It ranges from a regular flysch sequence to an ophiolitic mélange. It is difficult to put a boundary between the flyschoid Maden complex and the overlying ophiolitic mélange (Yüksekova complex or the Güleman ophiolite).

The Kırkgeçit Formation occupies large areas southeast of Van, where it lies unconformably over the Bitlis metamorphic rocks, the Yüksekova complex and the Hakkari complex. It consists of siliciclastic turbidites with extensive olistostrome horizons (Perinçek 1990). Scarce fossils indicate a Late Eocene to Early Miocene age for the Kırkgeçit Formation. Post-Miocene tectonics has resulted into the imbrication of the Kırkgeçit Formation with the underlying units.

Autochthonous sequence of SE Anatolia (Arabian Platform)

An account of the stratigraphy of the Arabian Platform as exposed in the anticlines south of Hakkari is given in the following. The authochthonous sequence (Ketin 1980) is well exposed in two faulted anticlines along the Zap River between Hakkari and Çukurca (Rigo de Rhigi & Cortesini 1964) the Great Zap anticline in the north and the Çukurca anticline in the south (Fig. 1). The anticlines are major regional east–west-trending structures with half wavelengths of 10–15 km, and extend along strike for over 100 km. Their southern margins are cut by thrust faults. The Great Zap and Çukurca anticlines expose a thick sedimentary sequence from Early Cambrian to Eocene, albeit with major gaps. Clastic rocks dominate the Cambrian to Carboniferous (Janvier *et al.* 1984) sequence, whereas the Permian (Köylüoglu & Altiner 2001) to Eocene sequence is largely formed by shallow marine carbonates. The lowermost authochthonous sequences in the core of the Great Zap anticline are medium to thickly bedded sandstones and siltstones belonging to the Derik Group. In the Great Zap anticline this group has a minimum thickness of 600 m and, based on scarce fossils, is of Early Cambrian age (Perinçek 1990; Yılmaz & Duran 1997). The Middle Cambrian dolomites and limestones of the Koruk Formation conformably overlie the arenites of the Derik Group. The Koruk Formation is equivalent to the Çaltepe Limestone in the Taurides. It is in turn overlain by yellowish brown siltstone, sandstone, and shale intercalation of the Seydisehir Formation of Late Cambrian–Ordovician age, which forms the core of the Çukurca anticline farther south. The Seydisehir Formation is unconformably overlain by the strikingly variegated, thickly bedded quartzites of Upper Devonian age belonging to the Yıgınlı Formation. The Late Devonian age is based on fish fossils (Janvier *et al.* 1984). The quartzites show strong current bedding and have thin shale and siltstone interlayers, and have a measured thickness of 295 m. The quartzites of the Yıgınlı Formation are conformably overlain by the shale, sandstone, sandy dolomite and limestone of the Köprülü Formation. The Köprülü Formation straddles the Devonian-Carboniferous boundary (Perinçek 1990; Yılmaz & Duran 1997) and has a thickness of about 200 m. The Upper Devonian–Lower Carboniferous Köprülü Formation is unconformably overlain by a thick carbonate sequence of Late Permian age. This Tanin Group has a thickness of nearly 1000 m, and consists of dark, bituminous, limestone and dolomitic limestone locally with chert nodules. A rich foraminifera fauna indicates the presence of all the Upper Permian stages from Murgabian to Dorashamian (Köylüoglu & Altıner 1989). The dark Upper Permian carbonates are overlain by purple, green, yellow shale, siltstone, shaley and lithographic limestone of Early Triassic age belonging to the Çıglı Group. The Çıglı Group has a thickness of about 500 m, and is conformably overlain by the thickly bedded, neritic limestone and dolomite of the Cudi Group of Middle Triassic to Early Cretaceous age. The thickness of the Cudi Group increases from west to east, and in the Hakkari-Çukurca region is more than 1000 metres. The youngest ages from the Cudi Group are Aptian-Albian, however, in many regions the Lower Cretaceous sequence is eroded, and the Upper Cretaceous rests unconformably over the older formations (Perinçek 1990). In the northern margin of the Great Zap anticline the neritic carbonates of the Cudi Group are unconformably overlain by the shaly pelagic limestones of the Sayındere Formation, about 200 m thick. A rich pelagic foraminifera fauna in the limestones indicates a Campanian age for the Sayındere Formation. The Sayındere Formation is unconformably overlain by the Campanian–Lower Paleocene sandstone, shale and marl of the Germav Formation. In several localities south of Hakkari, the Sayındere Formation is eroded and the Germav Formation rests directly on the neritic carbonates of the Cudi Group. The Lower to Upper Eocene Midyat Group unconformably overlies the Germav Formation. The Midyat Group starts with red conglomerates and sandstones, and passes up into thinly to thickly bedded limestones locally with chert nodules and interlayers. The Midyat Group is tectonically overlain by the allochthonous Hakkari complex along the frontal thrust. Slivers of Miocene continental sandstone, siltstone and mudstone (Selmo Formation) indicate a Miocene and younger age for the thrusting (Perinçek 1990).

New geological observations, metamorphic data and age constraints

Cross-sections in the Eastern Bitlis complex

Hakkari section. The easternmost cross-section runs along the main road from Van to Hakkari and Çukurca. From Van towards the SE, Oligo–Miocene sediments of the Kırkgeçit Formation are crossed, that exhibit phenomena of late tectonic movements typifying in the whole region. The Cenozoic and recent deformation led to faulting and block tilting. This sequence overlies Cretaceous ophiolitic coloured mélanges, with a serpentinitic and shaly matrix that contain large limestone blocks (Yüksekova fm). The contacts of the Oligo–Miocene sediments on the Cretaceous mélange are reported as transgressional although near Van thrusting of Cretaceous mélange and Eocene sequences is evidenced.

Between Baskale and Hakkari, SW of the Yüksekova junction, the rocks of the Urse Formation consist of silvery slates that show excellent kink bands (Fig. 2a) deformation patterns, which relate to metamorphism. Nearby, volcanoclastic and volcanic rocks show a bluish tint. While arkosic metasediments did not show any evident macroscopic trace of a low-grade HP-LT metamorphism the meta-volcanics contain blue amphibole. The blueschists of the Urse Formation are overlain by non-metamorphic Eocene flysch-type sediments (Fig. 2b).

Gevas – Çatak – Narli section (Fig. 3). Starting from Van, the first observation of the Northern contacts of the Bitlis complex is exposed around Gevas. Q4 There, the so-called Gevas ophiolite (Yilmaz 1978) is actually an ophiolitic mélange with a serpentinitic matrix that contains blocks of gabbros, basaltic rocks, cherts, limestones, and radiolarites. This mélange clearly dips southwards below the metamorphic sediments of the Bitlis complex with an angle of *c.* 20–30° (Fig. 4). The rather flat-lying contact is easily recognized by an alignment of springs. Strongly deformed and brecciated rocks of both complexes dominate the contact: the ophiolitic mélange and the overlying Bitlis metamorphics. Inspection of the contact at several locations however revealed that between the ophiolitic mélange and the Palaeozoic marbles of Çadir dag a typical rock sequence consisting of metasandstones and reddish marly calcitic marbles as well as marbles with chert layers occur. The reddish marly marbles resemble ‘couche rouge’-type sediments. This rock sequence resembles in many aspects the Cretaceous assemblages found in the Western Taurides. A cross-section east of Gevas (Fig. 4b) exhibits radiolarites of the mélange complex in direct steep contact with mylonitic marbles (Fig. 5a). These marble-mylonites are part of a metamorphic marble-schist sequence that typically occurs at the base of the Triassic sequence. In the investigated area the metamorphic sequence comprises calcareous and dolomitic marble seams in a greyish chlorite albite schist sequence. In some metapelitic layers phengite and chloritoid occur. Upward in the sequence the amount of

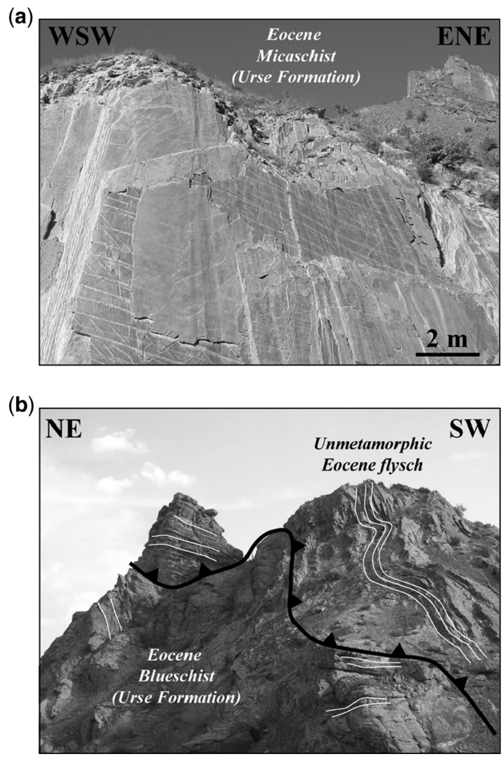

Q10

Fig. 2. Photographs of metamorphic rocks of the Eocene Urse Formation along the Bashkale Hakkari road. Top: slaty micaschist with kink bands. Bottom: Tectonic contact between Eocene Urse blueschists and Eocene flysch type clastic sediments.

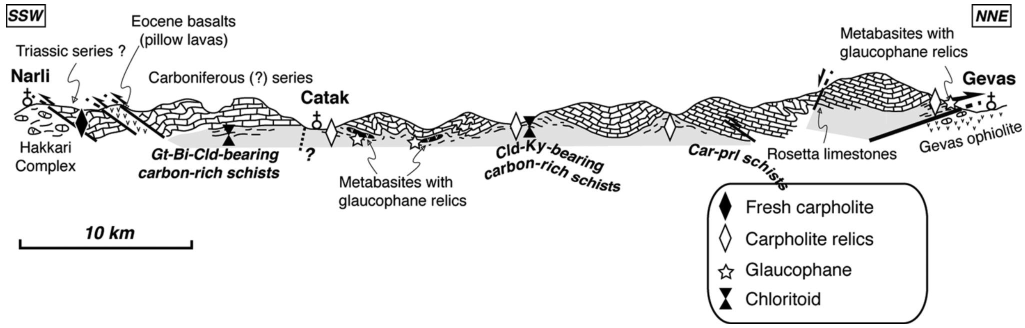

Fig. 3. Cross-section along the Çatak valley in the Eastern part of the meta-sedimentary cover of the Bitlis complex. Mafic and metapelitic rocks exhibit relicts of a HP-LT metamorphic event throughout the section.

dolomitic marbles diminishes and thin tuffitic mafic layers are intercalated within the schists. The mafic layers may also become more substantial and are composed of chlorite, epidote, amphibole and albite. In the uppermost part of the schist-marble sequence the mafic layers show intercalation of greenschist and blueschists (Fig. 5b). The blueschists contain albite, chlorite, glaucophane and epidote (Fig. 5c). The schist-marble sequence is conformably overlain by Megalodon (Fig. 5d) bearing massive grey marbles of possible Triassic age. Another section across the contact shows strongly deformed serpentinites that are capped by lysvenitic layers. Above these, light grey marbles

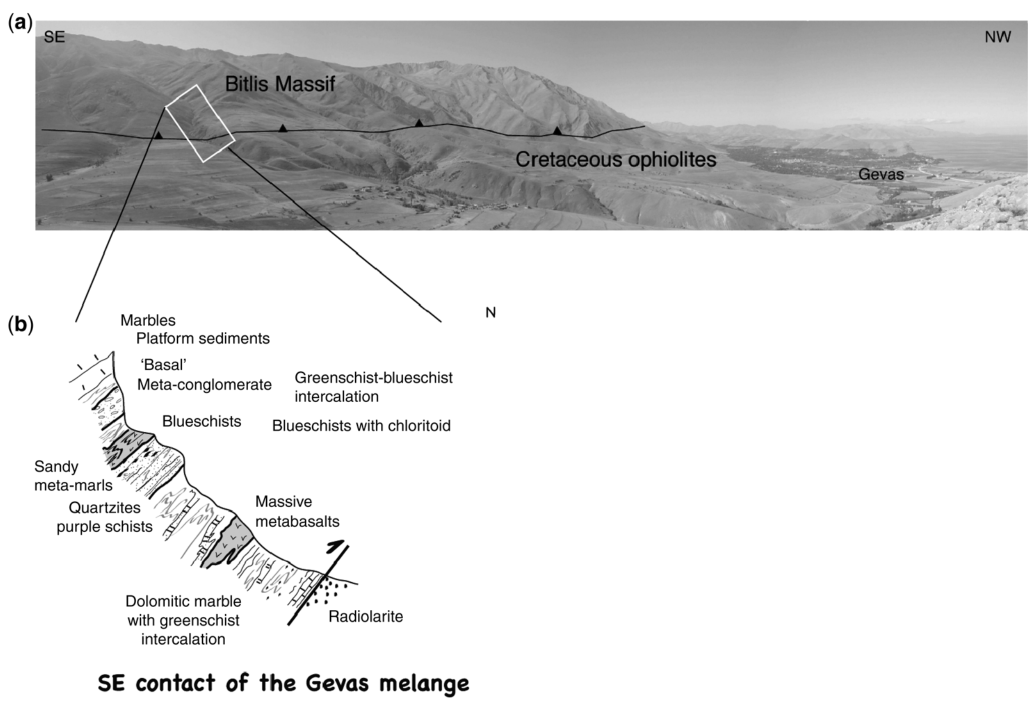

Fig. 4. (**a**) Photograph of the inverted contact putting the sediments of the Bitlis metamorphic complex over the mélange sequence of Gevas. View westward from NE. The village of Gevas is located at the right margin of the image. The box indicates the location of the section (b) taken over the tectonic contact. (**b**) Section trough the inverted tectonic contact Gevas mélange – Bitlis complex. At the base mylonitic dolomite marbles tectonically overlies radiolarian cherts. These grade into metabasites, schists, quartzites and, finally meta-conglomerate at the base of the Bitlis marbles. In the schistose part of the section blueschists occur.

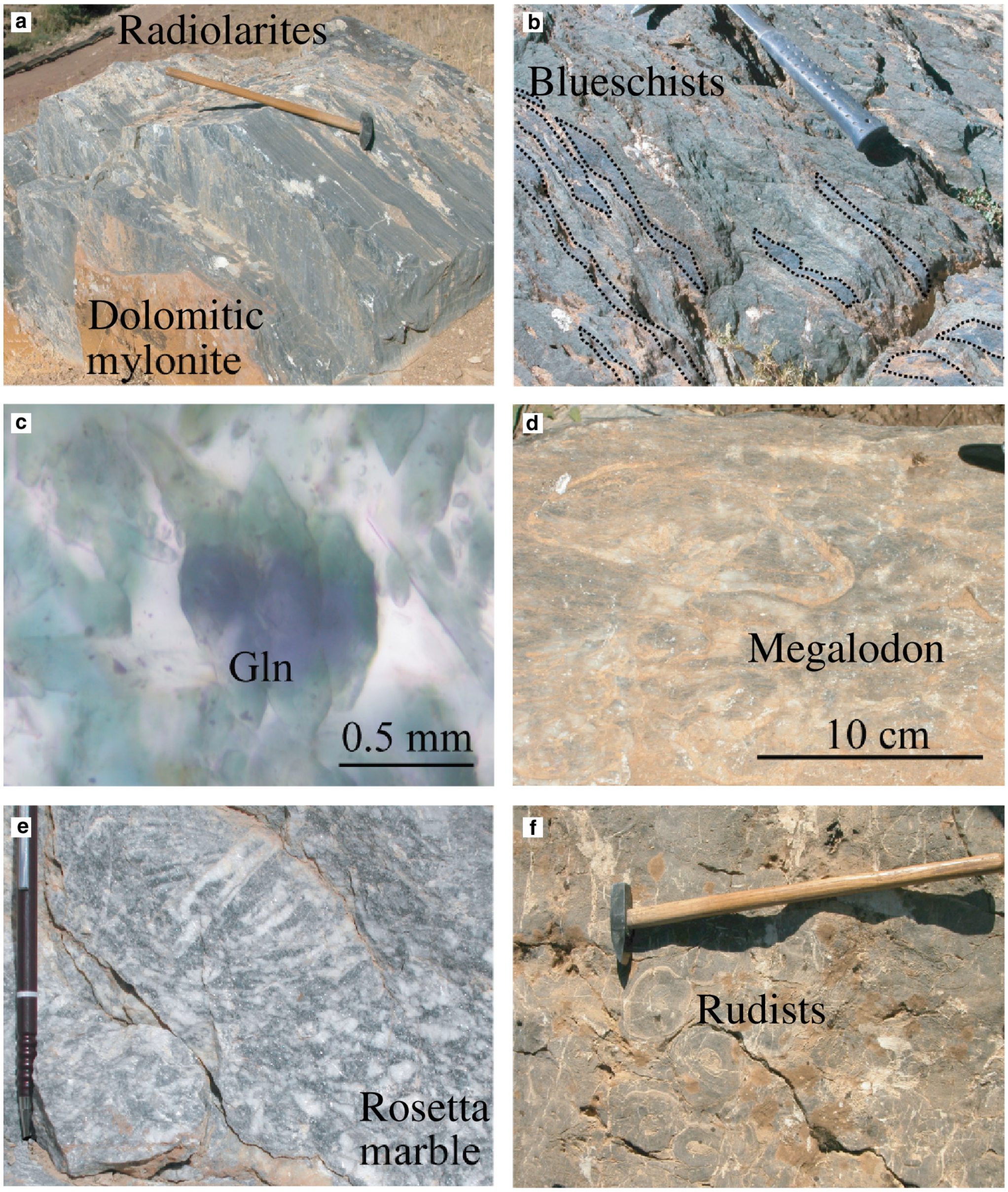

Colour online/ colour hardcopy

Fig. 5. Photographs (**a**) Mylonitic marbles at the base contact of the Bitlis with the Gevas complex. (**b**) Blueschist and greenschists, intercalated within the marbles. (**c**) Microphotograph of glaucophane rimmed by blue-green amphibole. (**d**) Triassic (?) Megalodon occurring in marbles of the Bitlis complex (Fig. 4b top left). (**e**) Calcitic rosetta (pseudomorphs after aragonite?) from the Bitlis marbles. (**f**) Cretaceous Rudist of Arabian faunal affinity (Özer 2005) found in limestones of the Gevas complex.

with whitish elongated calcite aggregates occur. Some of these aggregates show fibrous calcite, possibly pseudomorphs after aragonite (Fig. 5e). To some extent this resembles the upper Cretaceous 'rosetta' type marbles with their conspicuous cherty layers. Overlaying these rocks dark grey Permian marbles occur. A third section exhibits cataclastic contact relations. However, between the Permian Bitlis marbles and the ophiolite complex again a conspicuous sequence resembling closely the Cretaceous Tütü formation occurs. This metamorphic sequence contains relics of carpholite fibres, this again points to a low-grade high-pressure metamorphism. The limestone blocks within the Gevas ophiolitic mélange revealed rudists (Fig. 5f) that according to Özer (2005) show an Arabic facies affinity.

Entering the Çatak valley the first outcrops of the Palaeozoic marbles show strong cataclastic disruption and earlier ductile folding. These marbles are calcitic but show in some places relict whitish crystals that might have formed as sedimentary aragonite (Fig. 5e). In ductile shear bands around these rosetta-forming aggregates, fibrous calcite replaces metamorphic aragonite. These fibrous features are a clear hint to a low-grade HP-LT overprint close to the base of the Bitlis metamorphic complex. Intercalated with these Palaeozoic marbles, a sequence of black to silvery schist with mafic intercalations occur some 5 km southward, near Kayabogaz. In those schists, we identified the very first occurrence of carpholite relics in Eastern Anatolia. In these rocks carpholite has reacted to form chloritoid and quartz. Sometimes kyanite can be found in these chloritoid bearing rocks. The associated mafic rocks exhibit a bluish tint and glaucophane was found in thin section from these meta-basic intercalations.

Further downstream of the Çatak valley the series are strongly disrupted by complex folding and thrusting. The general structure is an open folding superimposed on overturned south vergent folded structures (Fig. 3).

Along this cross-section, the Bitlis metamorphic complex exposes only meta-sediments of upper Palaeozoic to Mesozoic sequences. North of Çatak spectacular chloritoid-bearing rocks with crystal sizes up to 2–3 cm are exposed. South of Çatak near Narli chloritoid-garnet-bearing parageneses occur in the metapelitic rocks. These higher-grade metapelites and their marble envelope are locally thrust on top of non-metamorphosed Eocene pillow lavas. Below this tectonic sliver, steep and strongly folded Palaeozoic to Permo-Triassic marbles forms the southern frontal part of the Bitlis complex. Along the Çatak River, the marbles contain fresh carpholite without chloritoid.

Metamorphic evolution

In the Bitlis cover (Fig. 6) silvery Al-rich metapelitic schists, intercalated with calcareous marbles, generally contain the assemblage chlorite-phengite-quartz. Along the frontal (south) and basal parts the assemblage carpholite-chlorite-phengite-quartz occurs. In rare cases pyrophyllite-chlorite-carpholite assemblages testify prograde relicts. In internal parts of the nappe complex most of the carpholite has reacted to form chloritoid and only carpholite relics included in quartz veins and nodules remain. The mineral stable assemblage is chloritoid-phengite-quartz-chlorite sometimes associated with paragonite. A few samples contain kyanite and chloritoid, others chloritoid and epidote and one sample containing garnet together with chloritoid, chlorite and phengite was found. Mafic rocks associated with these metapelites contain glaucophane and testify blueschist metamorphic conditions.

At regional scale the distribution of Fe, Mg-carpholite and glaucophane documents the extent of high-pressure low-temperature metamorphism all over the meta-sedimentary part of the Eastern Bitlis complex. Up to now we were not able to identify a similar HP metamorphism in the crystalline basement rocks. A first report on eclogites was given from the central part of the Bitlis complex at Mt Gablor (Okay *et al.* 1985) south of Mus. There, eclogites occur within garnet mica schists and contain kyanite. P–T estimates are reported with temperatures between 600° and 650 °C at 1.0 to 2.0 GPa. Based on findings of eclogite pebbles in Lower Palaeozoic micro-conglomerates a Pan African age was assumed for these eclogites (Göncüoglu *et al.* 1997).

Both high-pressure index minerals, glaucophane in metabasites and carpholite in metapelites can only be used for a rough estimate of the P–T conditions (e.g. Oberhänsli *et al.* 1995, 2001). Therefore we apply the multi-equilibrium approach developed and tested for chlorite-phengite-quartz bearing meta-sediments (Vidal *et al.* 1999; Vidal & Parra 2000; Parra *et al.* 2002; Rimmele *et al.* 2005). Fe, Mg-carpholite occurs overall the schist in the Bitlis complex (Fig. 6). Microprobe analysis document a homogenous chemical composition of Fe, Mg-carpholite (Table 1) with a relatively high Mg-content (X_{Mg}=0.65 – 0.70) in marbles (Fig. 7), and a lower Mg-content (X_{Mg}=0.33 – 0.50) in metapelitic schists. Chloritoid (Table 2) always shows significantly higher Fe contents (X_{Mg}=0.05 – 0.35) (Fig. 7). Thus the Fe-Mg partitioning coefficient $[K_D=(\mathrm{Fe/Mg})_A/(\mathrm{Fe/Mg})_B]$ for a carpholite/chloritoid pair is equal to 8. This K_D value is similar to those reported in the literature for the same rock-type and the equivalent P–T conditions (Crete: Theye *et al.* 1992; Oman: Vidal & Theye 1996, Alps: Bousquet *et al.* 2002).

Using microprobe analyses and recalculated end members of chlorite such as clinochlore, daphnite, sudoite and amesite as well as white mica such as celadonite, pyrophyllite and muscovite (Tables 3 & 4) it is possible to calculate P–T conditions for each chlorite-phengite mineral pair. Calculated P, T conditions indicate P=8–10 kb and T=320 °C for the prograde relicts, P=10–11 kb and T=350 – 400 °C for peak conditions and a wide distribution of temperatures (T: 370 – 480 °C) at lower

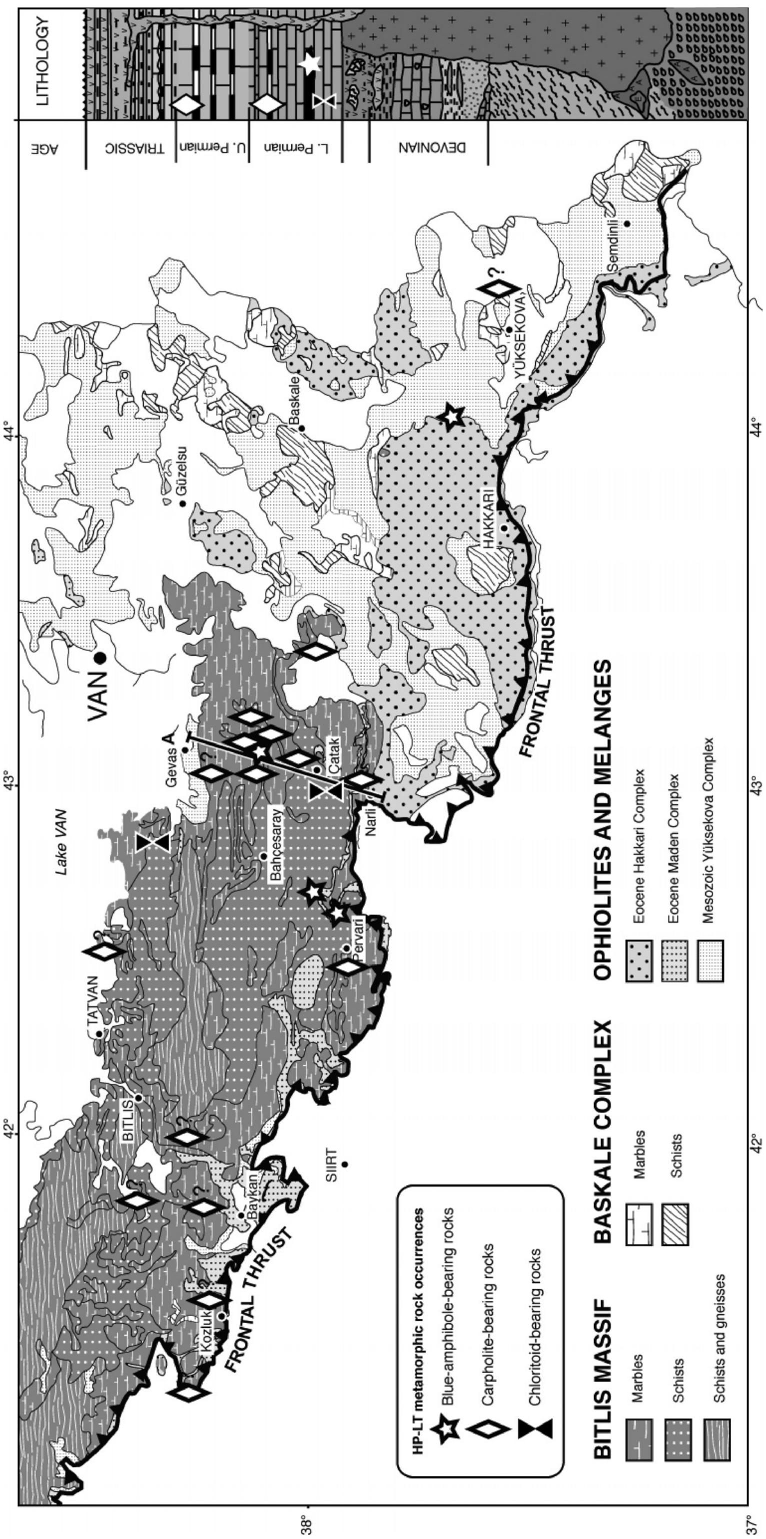

Fig. 6. Geological map of the eastern Bitlis complex (modified after the MTA 1:500 000 maps Cicre & Van). The distribution of HP-LT index minerals throughout the Eastern Bitlis complex and in the Eocene Urse Formation is indicated. Right side: Schematic lithostratigraphic column (modified after Göncüoglu & Turhan 1984).

Table 1. *Representative electron microprobe analyses of HP-LT index minerals Fe-Mg carpholite and glaucophane. All electron microprobe analyses using natural and synthetic mineral standards at standard conditions (15 kV, 20 nA) were performed on Cameca SX 100 at GFZ Potsdam and at CAMPARIS Paris VI*

Sample	VAN 7 car	VAN 7 car	VAN 7 car	VAN 11 car	VAN 41 car	VAN 41 car	Sample	VAN 55 glauc	VAN 55 glauc	VAN 55 bl-gn a
SiO_2	37.62	38.19	38.44	42.46	39.35	39.32	SiO_2	58.18	57.84	48.81
Al_2O_3	31.81	32.08	32.33	29.60	32.29	32.36	TiO_2	0.09	0.21	0.63
FeO	13.58	12.16	11.50	10.45	7.29	7.70	Al_2O_3	4.54	2.35	8.98
MnO	0.12	0.03	0.16	0.20	0.14	0.10	FeO	16.00	17.56	6.54
MgO	5.01	5.62	5.87	5.89	8.78	8.80	MnO	0.15	0.11	0.17
F	0.11	0.61	0.86	0.08	2.45	1.80	MgO	11.36	11.88	18.46
Total	88.25	88.69	89.15	88.68	90.30	90.07	CaO	0.49	1.17	12.31
							Na_2O	6.95	6.82	1.75
							K_2O	0.00	0.02	0.21
							Total	97.77	97.97	97.86
	Structural formula							Structural formula based on 13 cations Q11		
Si	2.00	2.02	2.02	2.23	2.03	2.02	Si	8.04	8.06	6.82
Al	1.99	2.01	2.02	1.99	1.99	1.98	Ti	0.01	0.02	0.07
Fe^{3+}	0.01	0.00	0.00	0.01	0.01	0.02	Al	0.74	0.39	1.48
Fe^{2+}	0.60	0.54	0.51	0.49	0.31	0.31	Fe	1.85	2.05	0.76
Mn	0.01	0.00	0.01	0.01	0.01	0.00	Mn	0.02	0.01	0.02
Mg	0.40	0.45	0.46	0.50	0.68	0.68	Mg	2.34	2.47	3.85
F	0.02	0.10	0.14	0.01	0.41	0.29	Ca	0.07	0.17	1.84
							Na	1.86	1.84	0.47
X_{Mg}	0.397	0.451	0.473	0.501	0.684	0.681	K	0.00	0.00	0.04

pressures (P: 3–6 kb) for the retrograde evolution (Fig. 8). These observations from Bitlis meta-sediments fit well with those made in Tethyan meta-sediments in Western Turkey: the Lycian nappes (Rimmele *et al.* 2002) and the Afyon Zone (Candan *et al.* 2005).

Age of metamorphism

Phengites from carpholite bearing metasediments from the Çatak valley were dated by laser $^{40}Ar/^{39}Ar$ method. Small amounts of pure phengite separated from carpholite fibbers in quartz exudates

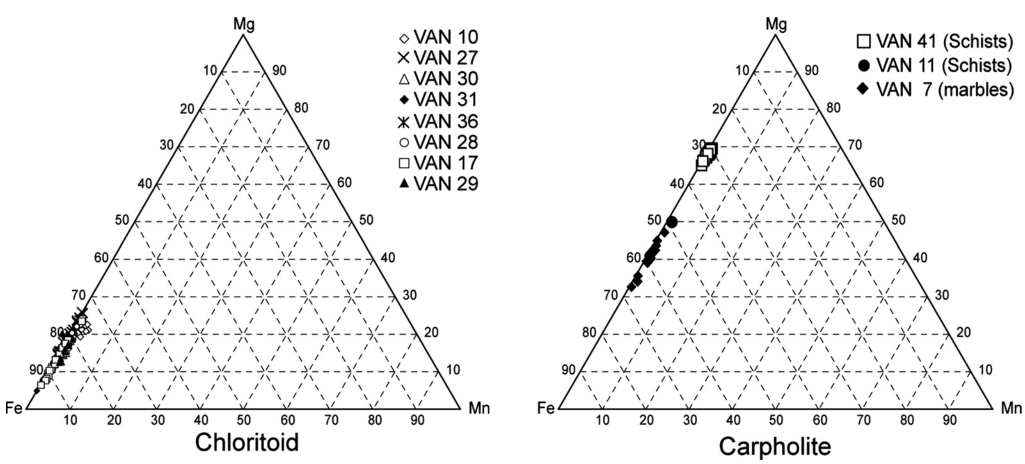

Fig. 7. Composition of carpholite and chloritoid from the Bitlis meta-sediments. As generally observed chloritoid is more iron rich than associated carpholite. The data presented fits well with data reported from Western Turkey (Lycian nappes and Afyon zone).

Table 2. *Representative electron microprobe analyses of chlorites with temperature estimates based on Jowett (1991). Mineral associations are indicated; sample with corresponding numbers and sequential number of analyses indicate mineral pairs*

Sample	Van 10		Van 27		Van 29	Van 36		Sample	Van 36	
Assemblage	chl-chd		chd-chl-phg		Chd-chl	gt-chl-chd-phg		Assemblage	gt-chl-chd-phg	
Anal n°	4	5	40	44	233	54	56	anal n:	47	49
SiO_2	24.57	24.50	24.63	25.12	24.37	24.65	24.76	SiO_2	36.72	37.49
TiO_2	0.09	0.02	0.19	0.00	0.23	0.02	0.04	TiO_2	0.15	0.00
Al_2O_3	41.06	39.39	40.91	41.48	39.87	41.54	41.61	Al_2O_3	21.16	21.37
FeO	23.28	25.86	24.69	24.54	25.09	23.99	25.27	FeO	33.78	35.73
MnO	0.99	0.39	0.21	0.00	0.27	0.00	0.01	MnO	3.08	0.00
MgO	3.42	3.38	2.86	3.10	2.51	2.84	3.07	MgO	0.73	2.07
CaO	0.10	0.00	0.06	0.01	0.07	0.00	0.00	CaO	6.08	4.91
Na_2O	0.00	0.00	0.00	0.01	0.00	0.02	0.01	Na_2O	0.01	0.01
K_2O	0.01	0.08	0.02	0.03	0.00	0.00	0.02	K_2O	0.02	0.00
Sum	93.51	93.61	93.55	94.29	92.41	93.06	94.77	Sum	101.74	101.58
	Structural formula based on 6 oxygens								Structural formula based on 12 oxygens	
Si	1.99	2.00	2.01	2.03	2.03	2.02	1.99	Si	2.95	2.98
Ti	0.01	0.00	0.01	0.00	0.01	0.00	0.00	Ti	0.01	0.00
Al	3.93	3.79	3.94	3.96	3.91	4.01	3.93	Al	2.00	2.00
Fe^{3+}	0.07	0.21	0.06	0.04	0.09	0.00	0.07	Fe^T	2.27	2.37
Fe^{2+}	1.58	1.77	1.69	1.66	1.75	1.64	1.70	Mn	0.21	0.00
Mn	0.07	0.03	0.01	0.00	0.02	0.00	0.00	Mg	0.09	0.25
Mg	0.41	0.41	0.35	0.37	0.31	0.35	0.37	Ca	0.52	0.42
Ca	0.01	0.00	0.00	0.00	0.01	0.00	0.00	Na	0.00	0.00
Na	0.00	0.00	0.00	0.00	0.00	0.00	0.00	K	0.00	0.00
K	0.00	0.01	0.00	0.00	0.00	0.00	0.00			
$T^{Chd/Chl}$ °C (Vidal_al99)	416.8	392.5	466.2	488.8	no equil. (750)	538.1	533.2			

Table 3. *Representative electron microprobe analyses of phengite associated to chlorite of table 2. Mineral associations are indicated; sample with corresponding numbers and sequential number of analyses indicate mineral pairs*

Sample Assemblage	Van 9 chl-phg		Van 10 chl-chd		Van 11 chl-phg-car		Van 12 Chl-phg		Van 27 chd-chl-phg		Van 29 Chd-chl	Van 36 gt-chl-chd-phg		Van 113 chl-phg		Van 120 chl-phg	
Anal n:	63	65	84	85	42	50	28	37	38	45	231	61	63	61	142	182	192
SiO_2	26.15	26.71	26.66	26.96	25.19	25.65	25.18	25.58	25.72	28.21	23.64	24.24	25.55	24.64	24.83	27.44	27.08
TiO_2	0.02	0.00	0.00	0.00	0.00	0.00	0.06	0.00	0.00	0.09	0.22	0.04	0.07	0.07	0.02	0.02	0.02
Al_2O_3	20.90	21.24	24.53	23.89	24.88	25.44	20.72	21.02	23.50	26.48	22.03	23.47	21.70	21.95	22.07	21.03	21.22
FeO	25.45	25.84	17.80	17.47	17.74	17.73	29.36	27.66	23.85	19.47	32.54	26.46	26.52	30.33	29.79	21.43	21.22
MnO	0.24	0.39	0.17	0.15	0.09	0.18	0.25	0.07	0.06	0.05	0.10	0.17	0.08	0.14	0.09	0.19	0.16
MgO	14.25	15.02	18.63	19.16	17.81	18.32	12.51	13.76	15.67	12.77	8.92	13.58	14.73	9.88	10.68	17.02	17.45
CaO	0.04	0.00	0.03	0.11	0.05	0.05	0.04	0.05	0.07	0.01	0.07	0.00	0.00	0.00	0.03	0.01	0.01
Na_2O	0.01	0.03	0.00	0.01	0.04	0.01	0.00	0.05	0.00	0.00	0.00	0.01	0.04	0.02	0.02	0.02	0.00
K_2O	0.02	0.00	0.00	0.00	0.01	0.04	0.03	0.10	0.04	0.01	0.05	0.01	0.00	0.13	0.02	0.00	0.00
F	0.14	0.02	0.05	0.25	0.07	0.37	0.02	0.00	0.59	0.17	0.17	0.02	0.17	0.00	0.00	0.33	0.00
Sum	87.22	89.26	87.87	88.00	85.88	87.78	88.17	88.28	89.50	87.25	87.75	87.99	88.85	87.15	87.55	87.49	87.17
Structural formula based on 14 oxygens																	
Si	2.77	2.76	2.68	2.70	2.59	2.59	2.70	2.71	2.64	2.85	2.60	2.56	2.67	2.68	2.68	2.83	2.80
Ti	0.00	0.00	0.00	0.00	0.00	0.00	0.00	0.00	0.00	0.01	0.02	0.00	0.01	0.01	0.00	0.00	0.00
Al	2.61	2.59	2.90	2.82	3.02	3.03	2.62	2.62	2.84	3.15	2.86	2.92	2.68	2.82	2.81	2.56	2.58
Fe	2.26	2.24	1.49	1.47	1.53	1.50	2.63	2.45	2.05	1.64	2.99	2.34	2.32	2.76	2.69	1.85	1.83
Mn	0.02	0.03	0.01	0.01	0.01	0.02	0.02	0.01	0.01	0.00	0.01	0.01	0.01	0.01	0.01	0.02	0.01
Mg	2.25	2.32	2.79	2.86	2.73	2.76	2.00	2.17	2.40	1.92	1.46	2.14	2.30	1.60	1.72	2.62	2.69
Ca	0.00	0.00	0.00	0.01	0.01	0.00	0.00	0.01	0.01	0.00	0.01	0.00	0.00	0.00	0.00	0.00	0.00
Na	0.00	0.01	0.00	0.00	0.01	0.00	0.00	0.01	0.00	0.00	0.00	0.00	0.01	0.00	0.00	0.00	0.00
K	0.00	0.00	0.00	0.00	0.00	0.01	0.00	0.01	0.00	0.00	0.01	0.00	0.00	0.02	0.00	0.00	0.00
F	0.09	0.02	0.03	0.16	0.05	0.23	0.02	0.00	0.38	0.11	0.12	0.02	0.11	0.00	0.00	0.21	0.00
T^{Chl} °C (Jowett91)	338.3	341.3	357.6	364.8	390.8	392.1	362.4	359.7	379.9	387.9	392.9	406.0	368.6	369.0	370.8	315.8	327.7

Table 4. *Representative electron microprobe analyses of chloritoid and garnet. For chloritoid associated with chlorite (see Table 2) temperature were estimated following the method of Vidal et al. (1999). Mineral associations are indicated; sample with corresponding numbers and sequential number of analyses indicate mineral pairs*

Sample Assemblage	Van 9 chl-phg		Van 11 chl-phg-car		Van 12 Chl-phg		Van 27 chd-chl-phg		Van 36 gt-chl-chd-phg		Van 113 chl-phg		Van 120 chl-phg	
Anal n:	62	64	43	51	27	36	39	47	64	64	60	143	183	191
SiO_2	50.16	49.72	47.06	47.26	49.05	48.56	45.92	47.79	46.98	46.98	46.50	47.93	49.27	47.85
TiO_2	0.11	0.11	0.02	0.08	0.26	0.26	0.05	0.13	0.11	0.11	0.14	0.17	0.03	0.06
Al_2O_3	29.99	29.79	36.07	37.07	28.33	28.56	29.23	35.92	35.84	35.84	31.60	35.78	34.29	39.00
FeO	3.90	4.13	2.14	1.83	4.66	4.70	19.02	1.82	1.73	1.73	3.82	1.05	2.07	1.05
MnO	0.03	0.00	0.08	0.11	0.00	0.00	0.12	0.07	0.00	0.00	0.04	0.01	0.00	0.00
MgO	2.20	2.06	0.48	0.47	2.24	1.93	2.17	0.89	0.65	0.65	1.54	0.72	0.96	0.24
CaO	0.15	0.00	0.04	0.16	0.10	0.00	0.03	0.06	0.00	0.00	0.02	0.01	0.00	0.01
Na_2O	0.31	0.34	0.99	1.15	0.17	0.27	0.01	1.04	1.36	1.36	0.52	0.47	3.26	5.52
K_2O	9.31	9.61	7.48	7.72	10.70	10.88	0.00	8.88	9.26	9.26	7.88	8.75	3.96	0.84
F	0.24	0.15	0.12	0.18	0.00	0.00	0.03	0.39	0.00	0.00	0.00	0.00	0.00	0.13
Sum	96.15	95.75	94.35	95.85	95.50	95.16	96.55	96.60	95.93	95.93	92.06	94.88	93.84	94.57
Structural formula based on 11 oxygens														
Si	3.32	3.31	3.11	3.08	3.31	3.30	3.10	3.11	3.09	3.09	3.19	3.15	3.22	3.06
Ti	0.01	0.01	0.00	0.00	0.01	0.01	0.00	0.01	0.01	0.01	0.01	0.01	0.00	0.00
Al	2.34	2.34	2.81	2.85	2.26	2.29	2.33	2.76	2.78	2.78	2.56	2.77	2.65	2.94
Fe^T	0.22	0.23	0.12	0.10	0.26	0.27	1.07	0.10	0.10	0.10	0.22	0.06	0.11	0.06
Mn	0.00	0.00	0.00	0.01	0.00	0.00	0.01	0.00	0.00	0.00	0.00	0.00	0.00	0.00
Mg	0.22	0.20	0.05	0.05	0.22	0.20	0.22	0.09	0.06	0.06	0.16	0.07	0.09	0.02
Ca	0.01	0.00	0.00	0.01	0.01	0.00	0.00	0.00	0.00	0.00	0.00	0.00	0.00	0.00
Na	0.04	0.04	0.13	0.15	0.02	0.04	0.00	0.13	0.17	0.17	0.07	0.06	0.41	0.68
K	0.39	0.82	0.63	0.64	0.92	0.94	0.00	0.74	0.78	0.78	0.69	0.73	0.33	0.07
F	0.10	0.06	0.05	0.07	0.00	0.00	0.01	0.16	0.00	0.00	0.00	0.00	0.00	0.05

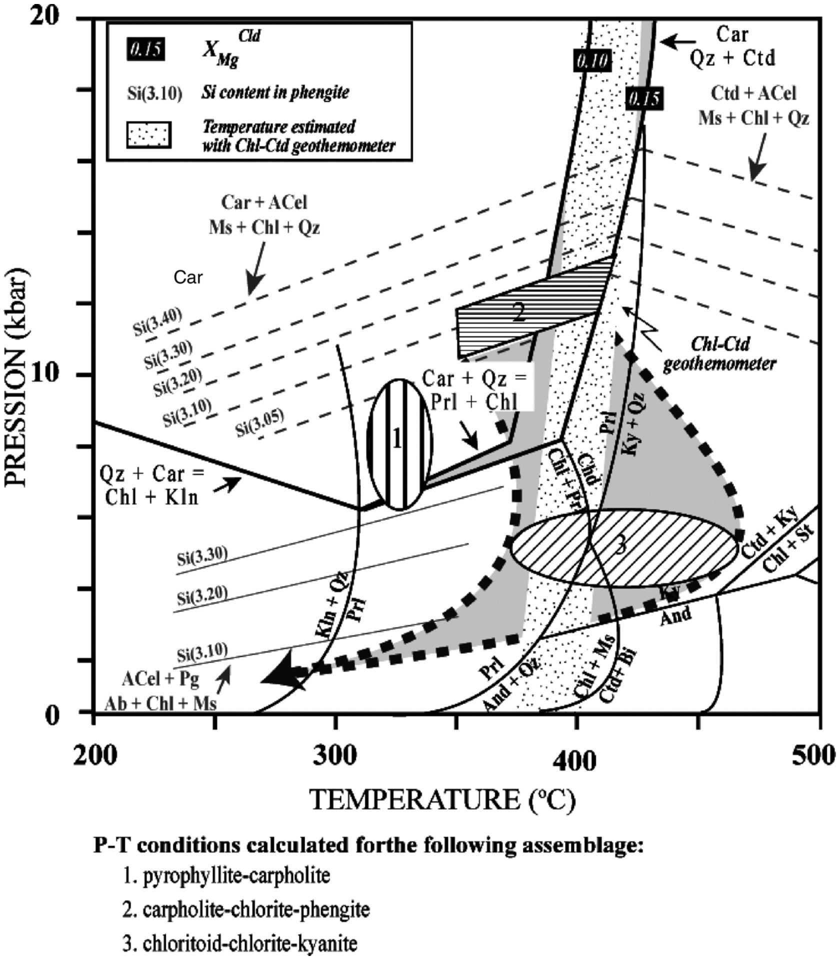

Fig. 8. Pressure temperature diagram for Al-rich carpholite bearing metapelites (after Oberhänsli *et al.* 1995; Bousquet *et al.* 2008) compiling the data for the Bitlis metapelites. 1, Prograde assemblages with pyrophyllite relicts; 2, Peak assemblages with carpholite and carpholite-chloritoid; 3, retrograde assemblages with chloritoid chlorite garnet and kyanite. The inferred retrograde paths range from isothermal decompression to moderate heating during decompression (see text).

with grain sizes in the range of 30–80 microns were hand picked and carefully washed by ultrasonic treatment in acetone, ethanol and distilled water. The samples were irradiated in the FRG-1 facility of the research reactor in Geesthacht (Germany). The neutron flux variation over the length of the sample capsule was monitored by Fish Canyon Tuff Sanidine (FC-3, 27.5 Ma; Ishizuka 1998; Uto *et al.* 1997) and calculated using a linear fit. Interference correction factors were obtained by analysing CaF_2 and K_2SO_4 irradiated together with the samples.

After irradiation the samples were loaded on a copper disc in the sample chamber. The system was baked for two days for reduction of atmospheric argon contamination. Mean blank values during the experiments for ^{40}Ar, ^{39}Ar, ^{37}Ar and ^{36}Ar were 1.46e-4, 7.32e-08, 8.95e-09 and 4.35e-06 respectively. During the experiment Ar was extracted from the samples using a 50 W CO_2 laser and isotopes were measured in a Micromass5400 spectrometer. Age spectra were produced from 3 respectively 7 grains that were heated by a moving beam with a diameter of 1600 microns for 90 seconds with 50 microseconds scan sped. Data have been corrected for blank, mass discrimination, ^{37}Ar and ^{39}Ar decay. They have been fitted on $^{36}Ar/^{40}Ar$ v. $^{39}Ar/^{40}Ar$ isochron plots (York 1969). Results are presented in Table 5 and Figure 9.

Table 5. *$^{40}Ar/^{39}Ar$ data for samples analysed at the University of Potsdam. The uncertainties on the total-gas ages include the uncertainty in the irradiation J parameter and are reported on 2σ level. The individual gas fractions are reported with analytical uncertainty on 1σ level, including the uncertainty on the J-value. Abbreviation: t.f.=total fusion*

Laser output (W)	$^{40}Ar/^{39}Ar$	$^{37}Ar/^{39}Ar$	$^{36}Ar/^{39}Ar$	K/Ca	$^{40}Ar^*$	$^{39}Ar_K$	$^{40}Ar^*/^{39}Ar_K$	Age (±1s) Ma
Van 75, phengitic mica J=0.00177								
0,012	139,06 ± 6,27	2,74 ± 2740,20	448,76 ± 28,29	0,21	4,89	0,06	6,82 ± 356,18	21,59 ± 1120,66
0,014	24,12 ± 0,22	0,06 ± 57,91	27,43 ± 0,72	10,16	66,43	2,77	16,02 ± 7,55	50,32 ± 23,39
0,016	21,72 ± 0,03	0,02 ± 17,22	5,15 ± 0,11	34,16	93,00	9,33	20,20 ± 2,25	63,21 ± 6,93
0,018	24,44 ± 0,05	0,01 ± 12,98	4,03 ± 0,10	45,33	95,13	12,39	23,25 ± 1,70	72,55 ± 5,22
0,020	24,56 ± 0,05	0,01 ± 5,88	2,67 ± 0,04	99,98	96,79	27,35	23,77 ± 0,77	74,15 ± 2,38
0,022	25,00 ± 0,04	0,01 ± 6,50	2,35 ± 0,05	90,49	97,22	24,76	24,31 ± 0,86	75,79 ± 2,63
0,024	25,74 ± 0,03	0,01 ± 8,85	3,90 ± 0,09	66,45	95,53	18,19	24,59 ± 1,16	76,65 ± 3,57
0,026	26,90 ± 0,16	0,05 ± 54,66	6,98 ± 0,48	10,76	92,36	2,95	24,85 ± 7,19	77,44 ± 21,93
t.f.	41,63 ± 0,24	0,07 ± 73,35	55,82 ± 1,24	8,02	60,40	2,20	25,14 ± 9,66	78,34 ± 29,44
Plateau age: 74.5 ± 1.5 Ma; total gas age: 73.3 ± 2 Ma								
Van 75A, phengitic mica J=0.00177								
0,014	71,59 ± 0,37	0,08 ± 75,13	185,37 ± 1,59	7,83	23,50	3,68	16,82 ± 9,81	52,79 ± 30,33
0,016	36,83 ± 0,10	0,02 ± 23,58	56,58 ± 0,56	24,95	54,61	11,73	20,11 ± 3,09	62,94 ± 9,50
0,018	28,25 ± 0,08	0,02 ± 16,16	17,27 ± 0,18	36,40	81,94	17,12	23,15 ± 2,12	72,24 ± 6,50
0,020	25,96 ± 0,16	0,01 ± 11,52	6,83 ± 0,13	51,07	92,23	23,80	23,95 ± 1,52	74,68 ± 4,65
0,022	25,57 ± 0,08	0,02 ± 15,13	5,26 ± 0,10	38,88	93,92	18,31	24,02 ± 1,99	74,91 ± 6,08
0,024	26,24 ± 0,09	0,03 ± 31,19	5,20 ± 0,20	18,86	94,16	8,89	24,71 ± 4,10	77,01 ± 12,52
0,026	25,68 ± 0,05	0,03 ± 26,03	4,92 ± 0,14	22,60	94,35	10,66	24,23 ± 3,42	75,54 ± 10,45
0,028	27,74 ± 0,22	0,08 ± 79,27	10,71 ± 0,53	7,42	88,63	3,50	24,58 ± 10,42	76,63 ± 31,81
t.f.*	59,40 ± 0,33	0,12 ± 119,66	111,03 ± 1,97	4,92	44,79	2,32	26,61 ± 15,78	82,81 ± 48,00
Plateau age: 74.4 ± 2.8 Ma; total gas age: 72.7 ± 3.4 Ma								

*t.f., total fusion.

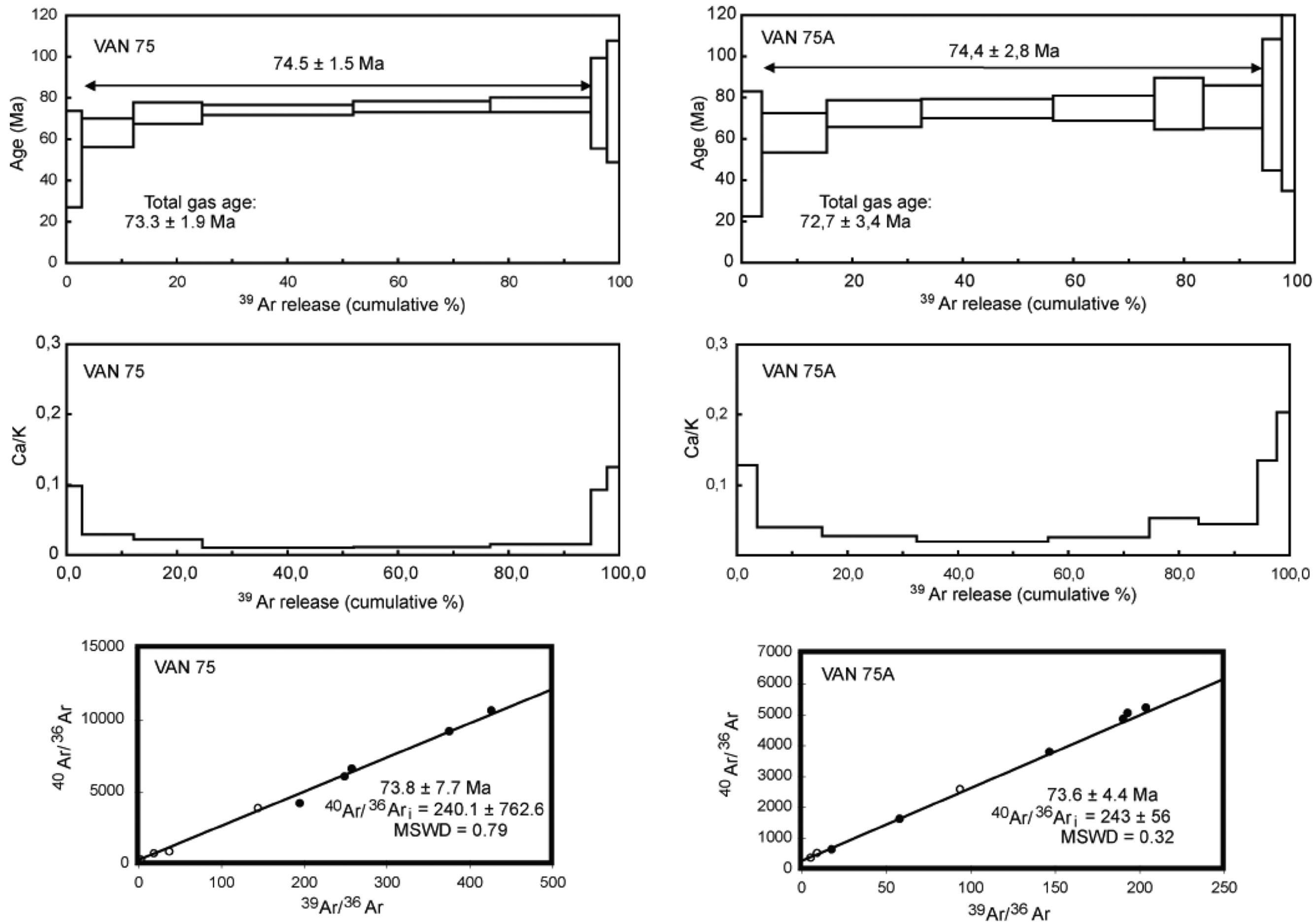

Fig. 9. $^{40}Ar/^{39}Ar$ phengite dating results from two carpholite bearing rocks of the metasedimentary cover of the Bitlis massif near Gevas.

Both samples are from the northernmost carpholite locality near Gevas. Both age spectra show a first step that is severely contaminated by atmospheric argon. Five respectively six gas fractions yield concordant apparent ages, which define plateau dates of 74.5 ± 1.5 Ma, and 74.4 ± 2.8 Ma. Isochron ages are similar to the plateau ages with intercept ages of 73.8 ± 7.7 Ma and 73.6 ± 4.4 Ma respectively (Fig. 9).

Excess argon may hamper the interpretation of $^{40}Ar/^{39}Ar$ phengite ages subjected to very high-pressure conditions (e.g. Li *et al.* 1994; Arnaud & Kelly 1995; Rufet *et al.* 1995). Strongly deformed, K-poor bulk compositions at low high-pressure conditions close to closure temperatures (350 ± 450 °C; Andriessen 1991) are barely suitable to incorporate excess argon in phengites (Oberhänsli *et al.* 1998; Sherlok & Kelly 2002). The Late Cretaceous age for the blueschist metamorphism in the Bitlis complex is compatible with the geological constraints as well as observations from the Lesser Caucasus, where H-P metamorphism is dated at 95-90 Ma (Rolland 2008). It is also younger than the H-P metamorphism of the Tavsanli zone in western Anatolia (e.g. Okay & Kelly 1994; Sherlok *et al.* 1999) but fits the age (K–Ar; 71.2 ± 3.6 Ma; Hempton 1985) of metamorphism from the Pütürge massif.

Discussion

As shown in figure 6, HP-LT metamorphism is distributed overall in the cover sequence of the eastern Bitlis complex.

Along the Çatak River, the marbles contain fresh carpholite without chloritoid. This clearly proves that the frontal part at the base of the western Bitlis complex experienced HP-LT metamorphism and that the temperatures never exceeded 450 °C since carpholite remained stable. On the contrary, the northern portion of the basal thrust experienced a slight heating after the HP-LT overprint, as attested by the reaction of carpholite retrogressed into chloritoid and quartz. Figure 8, a petrogenetic grid for Al-rich carpholite bearing metapelites, evidences low temperatures at elevated pressures for samples from the area where pyrophyllite was found. For samples with carpholite and carpholite relicts higher temperatures at high pressures are documented. Chloritoid bearing samples with carpholite relicts in quartz indicate similar conditions. Chloritoid samples without carpholite relicts indicate a wider range of temperatures at lower pressures. The stability of kyanite together with chloritoid indicates temperatures below 560 °C at 11 kb or 480 °C at 5 kb: the characteristic reaction, for Al-rich metapelites, chloritoid + kyanite = chlorite + staurolite (Spear & Cheney 1989) was never overstepped (Fig. 8). Garnet and epidote indicate decompression (Bousquet 2008). Form these observations we can conclude, that the retrogression from high-pressure low-temperature took place under conditions of isothermal decompression or at only a slightly elevated temperature conditions. The recorded temperature in metamorphic rocks of the Bitlis complex never exceeded 450 °C during the Mesozoic and Cenozoic evolution.

Along its northern contact of the Bitlis complex, Yilmaz (1978) described the Gevas complex as an ophiolite that was thrust over the Bitlis complex. Our investigations show that the Gevas complex is a mélange with a serpentinic matrix containing radiolarites and limestone blocks. The limestone blocks exhibit a rudist fauna with Arabic facies affinity, which is different from the rudist faunas of the Taurids (Özer 2005). The metamorphic sequence does not represent a metamorphic sole as inferred by Yilmaz (1978) but contains either relics of carpholite fibres or glaucophane. This points to a low-grade high-pressure metamorphism typical for cold geotherms only present in subduction related settings. Our investigation clearly shows that the Bitlis complex experienced a late Alpine subduction related history while the Gevas ophiolite material does not show any metamorphic overprint. Therefore the contact must be interpreted as late back thrust of the Bitlis complex towards the North.

The faunistic finding of Arabian facies affinity in the limestone blocks of the mélange contradicts the hypothesis of an obducted ophiolite block of northern provenance. In addition, HP-LT metamorphic conditions (≤450 °C) evidenced in the Bitlis complex but not in the Gevas ophiolitic mélange exclude obduction. It is obvious from petrography that the Bitlis complex and some Eocene formations experienced a subduction event and remained cold during its later geodynamic evolution. These facts were not considered in geodynamic evolution schemes published earlier (Yilmaz 1993; Sengör *et al.* 2003; Keskin 2003). Most of these scenarios do not consider the metamorphic evolution of the Bitlis complex at all.

Based on Cenozoic sediment evolution south of the Bitlis complex Yilmaz (1993) assumes during Late Maastrichtian to Early Eocene an intraoceanic subduction between a northern block and the Arabian Plate. This model accounts for Eocene to Oligocene subduction south of the Bitlis complex but does not detail the metamorphic evolution neither in the Bitlis complex not in the underlying Cenozoic nappes. Timing of the geodynamic evolution south of the Bitlis complex is well constrained in this model. However, geodynamically the nappe stacking of the 'metamorphic massifs' during Early Eocene is not well constrained (Yilmaz

1993, fig. 13). Later models (e.g. Sengör *et al.* 2003; Keskin 2003) focus on the geodynamic and volcanic evolution north of the Bitlis complex. While Sengör (2003) reflects on the tectonic building of the East Anatolian high plateau, Keskin (2003) focuses on its volcanic and magmatic evolution. In Sengörs model (Sengör *et al.* 2003, fig. 3) the Bitlis complex is thrust over the Arabian platform some time between Late Eocene and Middle Miocene without any clear geodynamic reason. In Keskin's model (Keskin 2003, fig. 3) the Bitlis complex is exhumed before Early Eocene and is part of a volcanic arc. The collision of the Arabian plate with the Bitlis Arc terminated during Late Oligocene–Early Miocene, while closure of the East Anatolian Accretion complex continued. At 11–13 Ma slab brake off followed since 6 Ma by asthenospheric upwelling is postulated (Sengör *et al.* 2003; Keskin 2003).

New geophysical observations in Eastern Anatolia infer seismic velocities smaller than expected for lithospheric mantle (Zor *et al.* 2003; Gök *et al.* 2007). Thus similarly to earlier models asthenospheric up welling following a slab break off event is assumed (e.g. Facenna *et al.* 2006; Barazangi *et al.* 2006). From seismic data (Gök *et al.* 2007) infers north directed major thrusts that fit well with our observations along the Gevas mélange.

To respect the metamorphic evolution and especially the preservation of HP-LT assemblages we propose a scenario (Fig. 10) that accounts for the Late Cretaceous (*c.* 74 Ma) metamorphic evolution. The Bitlis complex is routed northwards below the South-Armenian Block while its frontal parts are thrust southward over the Arabian platform and the Cenozoic complexes. Investigations of the Sevan-Akera suture zone in the Lesser Caucasus (Sosson *et al.* 2010) and new finding of HP assemblages along the ophiolitic suture near Stepanavan (Rolland *et al.* 2008) and its correlation to the Izmir Ankara Erzincan suture led us to assume that the Bitlis block collided with the South Armenian block during the Late Cretaceous.

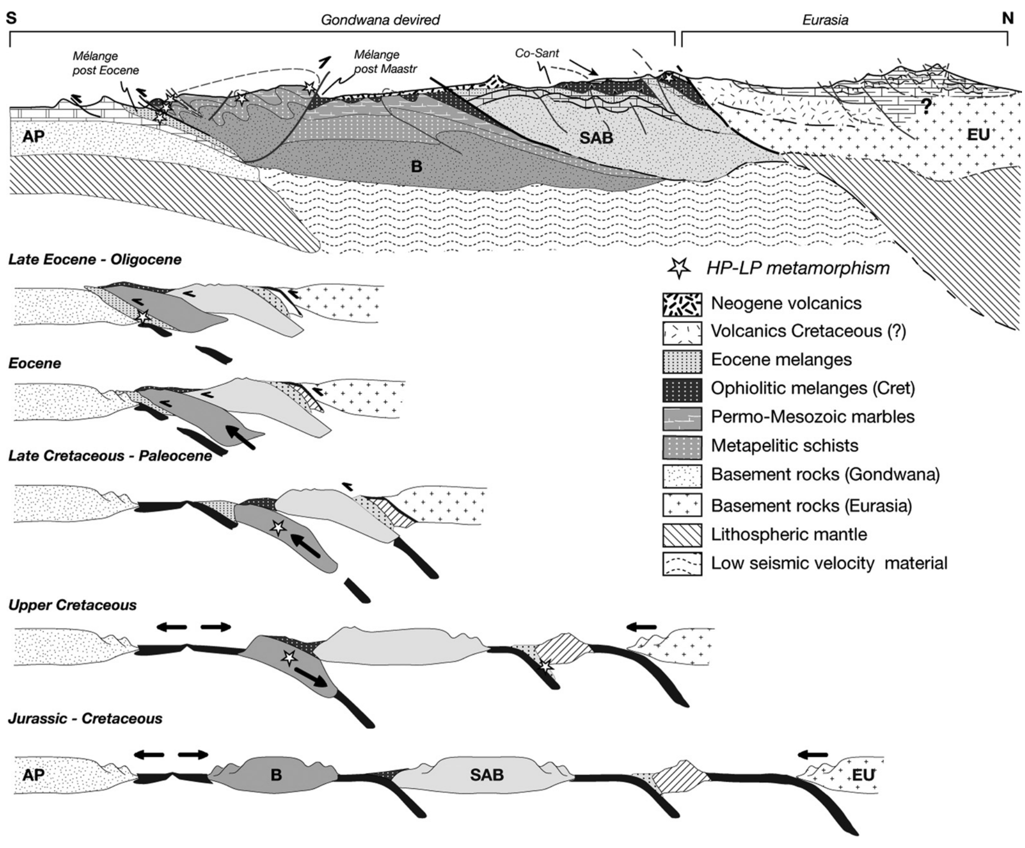

Fig. 10. Schematic geodynamic cross-section including data from 'MEBE Caucasus Group' by Sosson *et al.* (2010). In order to maintain cool conditions we consider a strong underthrust of the Arabian platform and separation of areas with asthenospheric upwelling for the Bitlis complex (see text).

This implies that the Bitlis complex was part of the Arabian platform and cannot be strictly correlated with the Tauride block. It separated from Arabia probably during Jurassic to Cretaceous time. After northward subduction the Bitlis complex had to be exhumed rapidly (supported by pyrophyllite relicts) probably already during Late Cretacous, since the Bitlis metamorphic units are imbricated with non-metamorphic Eocene pillow lava in the frontal part of the nappe complex (Fig. 1). To preserve its subtle HP-LT phases later significant heating must be excluded. This is possible if exhumation is rapid and the Bitlis complex further on remained close to the surface or if subduction processes are ongoing in the south as it is documented by blueschist assemblages in the Eocene Urse formation.

The non-metamorphic ophiolitic mélanges of the Yüksekova complex derive from the oceanic realm between the South Armenian and Bitlis blocks and were thrust over the exhuming Bitlis complex (Fig. 10). After collision of the Arabian plate with the Bitlis complex back thrusting led to the exhumation of basement rocks and the northern part of the Bitlis complex along Lake Van and the Yüksekova complex in Gevas. Our Interpretation with an Oligocene subduction of a mid oceanic ridge allows for later asthenospheric up welling without the need of subduction rollback and slab break off.

Conclusions

Petrological investigations in the eastern Bitlis complex clearly demonstrate subduction related HP-LT metamorphic conditions. These findings must be taken into consideration when reconstructing the geodynamic evolution of eastern Anatolia in front of the Arabian indenter, and especially for the delamination processes of the South Armenian block and its relation with recent volcanism. A first and obvious result is that the Gevas complex should not be considered as a complete ophiolite sequence but rather composes a serpentinitic mélange similar the Yüksekova complex. Now overturned, it overlays the Bitlis complex which exhibits relics of HP-LT metamorphism. Faunistic and petrographic investigations support an Arabian/Gondwanian origin for the Bitlis complex rather than a Tauride provenance. The fact that HP-LT parageneses are distributed over the whole of the Bitlis complex demonstrates that this complex experienced a subduction event and remained cold during its later geodynamic evolution. Geophysical data point to material with lower seismic velocities, interpreted as hot asthenospheric mantle situated just north of the Bitlis complex. Despite this, subtle HP-LT metamorphic assemblages are preserved indicating that after the subduction event no significant rise of temperatures has occurred.

The Bitlis complex is part of the complex Alpine belt with a collage of terranes and clearly more than one subduction zone. The blueschist metamorphism (*c*. 75 Ma) found distributed within the Bitlis complex points to a second subduction zone south of the major Izmir–Ankara–Erzincan–Sevan–Akera suture with a metamorphic H-P age of *c*. 90 Ma. The finding of blue amphibole and mica with in the Eocene mélanges south of the non-metamorphic Yüksekova ophiolitic mélange points to an even younger subduction type feature south of the Bitlis complex. Thus the region forming a high plateau in it status nascendii in eastern Anatolia composes a set of Gondwana derived blocks separated by oceanic domains that successively collided to with Eurasia.

We thank M. F. Brunet, E. Barrier and J. P. Cadet, all part of the MEBE team in Paris for their technical and financial support. M. Sudo and M. Timmerman supported work in the Ar lab. M. Sosson and J. Mosar inspired us in many discussions. The reviews by R. Klemd and Y. Rolland are highly acknowledged.

References

ANDRIESSEN, P. A. M. 1991. K-Ar and Rb-Sr age determinations on micas of impure marbles on Naxos, Greece: The influence of metamorphic fluids and lithology on the blocking temperature. *Schweizerische Mineralogische und Petrographische Mitteilungen*, **71**, 89–99.

ARNAUD, N. O. & KELLY, S. 1995. Evidence for excess Ar during high-pressure metamorphism in the Dora Maira massif (western Alps, Italy) using an ultra-violet laser ablation microprobe $^{40}Ar/^{39}Ar$ technique. *Contributions to Mineralogy and Petrology*, **121**, 1–11.

BARAZANGI, M., SANDVOL, E. & SEBER, D. 2006. Structure and tectonic evolution of the Anatolian plateau in eastern Turkey. *In*: DILEK, Y. & PAVLIDES, S. (eds) *Post-collisional Tectonics and Magmatism in the Mediterranean Region and Asia*. Geological Society of America, Special Paper, Boulder, CO, 463–473.

BORAY, A. 1975. Bitlis dolayının yapısı ve metamorfizması. *Turk Jeoloji Kurultai Bülteni*, **18**, 81–84.

BOUSQUET, R., OBERHÄNSLI, R. *ET AL*. 2008. Metamorphism of metasediments at the scale of an orogen: a key to the Tertiary geodynamic evolution of the Alps. *In*: FÜGENSCHUH, S. & FROITZHEIM, N. (eds) *Tectonic aspects of the Alpine-Dinaride-Carpathian System*. Geological Society, London, Special Publications, **298**, 393–411.

BOUSQUET, R., GOFFÉ, B., VIDAL, O., OBERHÄNSLI, R. & PATRIAT, M. 2002. The tectono-metamortphic history of the Valaisan domain from the Western to the Cental Alps: new constraints on the evolution of the Alps. *Geological Society, America, Bulletiin*, **114**, 207–225.

Çailayan, M. A., Önal, R. N., Sengün, M. & Yurtsever, A. 1984. Structural setting of the Bitlis Massif. *In*: Tekeli, O. & Göncüoglu, M. C. (eds) *Geology of the Taurus Belt. Proceedings of the International Symposium on the Geology of the Taurus Belt*, Ankara, 245–254.

Candan, O., Çetinkaplan, M., Oberhänsli, R., Rimmelé, G. & Akal, C. 2005. Alpine high-P/low-T metamorphism of the Afyon Zone and implications for the metamorphic evolution of Western Anatolia. *Lithos*, **84**, 102–124.

Faccenna, C., Bellier, O., Martinod, J., Piromallo, C. & Regard, V. 2006. Slab detachment beneath eastern Anatolia: a possible cause for the formation of the North Anatolian fault. *Earth and Planetary Science Letters*, **242**, 85–97.

Gök, R., Pasyanos, M. E. & Zor, E. 2007. Lithospheric structure of the continent–continent collision zone: eastern Turkey. *Geophysical Journal International*, **169**, 1079–1088.

Gök, R., Sandvol, E., Turkelli, N., Seber, D. & Barazangi, M. 2003. Sn attenuation in the Anatolian and Iranian plateau and surrounding regions. *Geophysical Research Letters*, **30**. **Q6**

Göncüoglu, M. C. 1984. Mus-Kızılagaç metagranitinin baikalasımı ve yası. *Maden Tektik ve Arama dergisi*, **99–100**, 72–83.

Göncüoglu, M. C. & Turhan, N. 1984. Geology of the Bitlis metamorphic belt. *In*: Tekeli, O. & Göncüoglu, M. C. (eds) *Geology of the Taurus Belt*. Procceedings of the International Symposium on the Geology of the Taurus Belt, Ankara, 237–244.

Göncüoglu, M. C. & Turhan, N. 1992. *Mus – I 33 paftası. 100 000 scale geological map series of Turkey*. Maden Tetkik ve Arama Genel Müdürlügü, Ankara.

Göncüoglu, M. C. & Turhan, N. 1997. Rock units and metamorphism of the basement and Lower Paleozoic cover of the Bitlis Metamorphic complex, SE Turkey. *In*: Göncüoglu, M. C. & Derman, A. S. (eds) *Lower Paleozoic Evolution in Northwest Gondwana.* Turkish Association Petroleum Geology, Special Publication, **3**, 75–81, Ankara. **Q7**

Göncüoğlu, M. C., Dirik, K. & Kozlu, H. 1997. General Characteristics of pre-Alpine and Alpine Terranes in Turkey: explanatory notes to the terrane map of Turkey. *Annales Geologique de Pays Hellenique*, **37**, *Geological Society, Greece*, 515–536, Athens.

Hall, R. 1976. Ophiolite emplacement and the evolution of the Taurus suture zone, southeastern Turkey. *Geological Society, America, Bulletin*, **87**, 1078–1088.

Hall, R. & Mason, R. 1972. A tectonic mélange from the Eastern Taurus Mountains, Turkey. *Journal Geological Society, London*, **128**, 395–397.

Helvaci, C. & Griffin, W. L. 1984. Rb-Sr geochronology of the Bitlis Massif, Avnik (Bingöl) area, S. E. Turkey. *In*: Dixon, J. E. & Robertson, A. H. F. (eds) *The Geological Evolution of the Eastern Mediterranean.* Geological Society, London, Special Publications, **17**, 403–413.

Hempton, M. R. 1985. Structure and deformation history of the Bitlis suture near Lake Hazar, southeastern Turkey. *Geological Society, America, Bulletin*, **96**, 233–243.

Horstink, J. 1971. The Late Cretaceous and Tertiary geological evolution of eastern Turkey. *1. Petroleum Kongresi*, 25–41.

Ishizuka, O. 1998. Vertical and horizontal variation of the fast neutron flux in a single irradiation capsule and their significance in the laser-heating $^{40}Ar/^{39}Ar$ analysis: case study for the hydraulic rabbit facility of the JMTR reactor, Japan. *Geochemical Journal*, **615**, 243–252.

Janvier, P., Lethiers, F., Monod, O. & Balkas, O. 1984. Discovery of a vertebrate fauna at the devonian-Carboniferous boundary in SE Turkey (Hakkari Province). *Journal Petroleum Geology*, **7**, 147–168.

Jowett, E. C. 1991. *Fitting iron and magnesium into the hydrothermal chlorite geothermometer. GAC/MAC/SEG Joint Annual Meeting (Toronto), Program with Abstracts*, **16**, A62.

Kellogg, H. E. 1960. *Stratigraphic report, Hazro area, petroleum district V. SE Turkey*. Maden Tektik ve Arama, Report. Ankara.

Keskin, M. 2003. Magma generation by slab steepening and breakoff beneath a subduction-accretion complex: an alternative model for collision-related volcanism in Eastern Anatolia, Turkey. *Geophysical Research Letters*, **30**, 1–4.

Ketin, S. 1980, Hakkari-Çukurca arasının büyük Zap suyu boyunca jeoloji kesiti. *In*: *Altınlı Symposium, Ankara*, 11–13.

Köylüoglu, M. & Altiner, D. 1989. Micropaléontologie (Foraminiféres) et biostratigraphie du Permien Supérieur de la région d'Hakkari (SE Turquie). *Revue Paléobiologie*, **8**, 467–503.

Lei, J. & Zhao, D. 2007. Teleseismic evidence for a break-off subducting slab under Eastern Turkey. *Earth and Planetary Science Letters*, **257**, 14–28.

Li, S., Wang, S., Chen, Y., Liu, D., Qiu, J., Zhou, H. & Zhang, Z. 1994. Excess argon in phengites from eclogite: evidence from dating of eclogite minerals by Sm-Nd, Rb-Sr, $^{40}Ar/^{39}Ar$ methods. *Chemical Geology*, **112**, 343–350.

Oberhänsli, R., Goffe, B. & Bousquet, R. 1995 Record of a HP-LT metamorphic evolution in the Valais zone: Geodynamic implications. *Bolletino del Museo Regionale delle Scienze naturali Torino*, **13**, 221–240.

Oberhänsli, R., Monié, P., Candan, O., Warkus, F. C., Partsch, J. H. & Dora, O. Ö. 1998. The age of blueschist metamorphism in the Mesozoic cover series of the Menderes massif. *Schweizerische Mineralogische und Petrographische Mitteilungen*, **78**, 309–316.

Oberhänsli, R., Partsch, J., Candan, O. & Çetinkaplan, M. 2001. First occurrence of Fe-Mg-carpholite documenting a high pressure metamorphism in the metasediments of the Lycian nappes, SW Turkey. *International Journal Earth Sciences*, **89**, 863–869.

Okay, A. I. & Kelley, S. P. 1994. Jadeite and chloritoid schists from northwest Turkey: tectonic setting, petrology and geochronology. *Journal of Metamorphic Geology*, **12**, 155–166.

Okay, A., Arman, M. B. & Göncüoglu, M. C. 1985. Petrology and phase relations of the kyanite-eclogites from Eastern Turkey. *Contributions to Mineralogy and Petrology*, **91**, 196–204.

Özer, S. 1992. Presence of rudist bearing limestone blocks derived from the Arabian Platform in Gevaş (Van) ophiolite. *Maden Tektik ve Arama Bulletin*, **114**, 75–82.

Özer, S. 2005. Two new species of canaliculate rudists (Dictyoptychidae) from southeastern Turkey *GEOBIOS-LYON*, **38**, 235–245.

Özkaya, S. 1982. Marginal basin ophiolites at Oramar and Karadas, SE Turkey. *Journal of the Geological Society, London*, **139**, 203–210.

Parra, T., Vidal, O. & Jolivet, L. 2002. Relation between deformation and retrogression in blueschist metapelites of Tinos island (Greece) evidenced by chlorite-mica local equilibria. *Lithos*, **63**, 41–66.

Perinçek, D. 1979. *Guidebook for Excursion 'B', Interrelations of the Arab and Anatolian plates.* 1st Geological Congress Middle East, Ankara.

Perinçek, D. 1990. Hakkari ili ve dolayının stratigrafisi, Güneudoğu Anadolu, Türkiye. *Türkiye Petrol Jeologları Derneği Bülteni*, **2**, 21–68.

Rigo de Righi, M. & Cortesini, A. 1964. Gravity tectonics in foothills structure belt of southeast Turkey. *American Association of Petroleum Geologists, Bulletin*, **48**, 1911–1937.

Rimmele, G., Jolivet, L., Oberhänsli, R. & Goffé, B. 2002. Deformation history of the high-pressure Lycian Nappes and implications for tectonic evolution of SW Turkey. *Tectonics*, **22**, 1007, doi: 10.1029/2001TC901041.

Rimmele, G., Parrra, T., Goffé, B., Oberhänsli, R., Jolivet, L. & Candan, O. 2005. Exhumation paths of high-pressure–low-temperature metamorphic rocks from the Lycian Nappes and the Menderes Massif (SW Turkey): a multi-equilibrium approach. *Journal of Petrology*, **46**, 641–669.

Rolland, Y., Billo, S., Corsini, M., Sosson, M. & Galoyan, G. 2008. Blueschists of the Amassia-Stepanavan Suture Zone (Armenia): linking Tethys subduction history from E-Turkey to W-Iran. *International Journal of Earth Sciences*, doi: 10.1007/s00531-007-0286-8.

Ruffet, G., Féraud, G., Ballèvre, M. & Kienast, J. R. 1995. Plateau ages and excess argon in phengites: an ^{40}Ar-^{39}Ar laser probe study of Alpine micas (Sesia Zone, Western Alps, northern Italy). *Chemical Geology*, **121**, 327–343.

Şengör, A. M. C. & Yilmaz, Y. 1981. Tethyan evolution of Turkey, a plate tectonic approach: *Tectonophysics*, **75**, 181–241.

Sengör, A. M. C., Özeren, S., Genç, T. & Zor, E. 2003. East Anatolian high plateau as a mantle supported, north–south shortened domal structure. *Geophysical Research Letters*, **30**, 8045.

Sengör, A. M. C., Ozeren, S., Genc, T. & Zor, E. 2003. East Anatolian high plateau as a mantle-supported, Q6 north–south shortened domal structure. *Geophysical. Research Letters*, **30**.

Şengün, M. 1993. Bitlis Masifi'nin metamorfizması ve örtü çekirdek ilişkisi. *Maden Tetkik ve Arama Dergisi*, **115**, 1–13.

Sherlok, S., Kelly, S., Inger, S., Harris, N. & Okay, A. 1999. ^{40}Ar-^{39}Ar and Rb-Sr geochronology of high-pressure metamorphism and exhumation history of the Tavsanli Zone, NW Turkey. *Contributions to Mineralogy and Petrology*, **137**, 46–58.

Sherlok, S. & Kelley, S. 2002. Excess argonevolution in HP-LT rocks: a UVLAMP study of phengite and K-free minerals, NW Turkey. *Chemical Geology*, **182**, 619–636.

Sosson, M., Rolland, Y. *et al.* 2010. Subductions, obduction and collision in the Lesser Caucasus (Armenia, Azerbaijan, Georgia), new insights. *In*: Stephenson, R. A., Kaymakci, N., Sosson, M., Starostenko, V. & Bergerat, F. (eds) *Sedimentary Basin Tectonics from the Black Sea and Caucasus to the Arabian Platform.* Geological Society, London, Special Publications, **340**, 329–352.

Spear, F. & Cheney, J. 1989. A petrogenetic grid for pelitic schists in the system SiO2-Al2O3-FeO-MgO-K2O-H2O. *Contributions to Mineraloy and Petrology*, **101**, 149–164.

Sungurlu, O. 1974. VI. Bölge kuzey sahalarının jeolojisi. *Türkiye İkinci Petrol Kongresi, Tebliğler*, Ankara, 85–107.

Theye, T., Seidel, E. & Vidal, O. 1992. Carpholite, sudoite and chloritoid in low-grade high-pressure metapelites from Crete and the Peloponnese, Greece. *European Journal of Mineralogy*, **4**, 487–507.

Tolun, N. 1953. Contributions à L'étude géologique des environs du sud et sud-ouest du Lac de Van. Turkey. *Mineral Research and Exploration Institution Bulletin*, **44/45**, 77–112.

Uto, K., Ishizuka, O., Matsumoto, A., Kamioka, H. & Togashi, S. 1997. Laser-heating ^{40}Ar/^{39}Ar dating system of the Geological Survey of Japan: System outline and preliminary results. *Bulletin of the Geological Society, Japan*, **48**, 23–46.

Vidal, O. & Parra, T. 2000. Exhumation paths of high-pressure metapelites obtained from local equilibria for chlorite-phengite assemblages. *Geological Journal*, **35**, 3–4.

Vidal, O. & Theye, T. 1996. Comment on 'Petrology of Fe-Mg-carpholite-bearing metasediments from NE Oman'. *Journal of Metamorphic Geology*, **14**, 381–386.

Vidal, O., Goffé, B., Bousquet, R. & Parra, T. 1999. Calibration and testing of an empirical chloritoid-chlorite Mg-Fe exchange thermometer and thermodynamic data for daphnite. *Journal of Metamorphic Geology*, **17**, 25–39.

Yigitbas, E. & Yilmaz, Y. 1996. New evidence and solution to the Maden complex controversy of the Southeast Anatolian orogenic belt (Turkey). *Geologische Rundschau*, **85**, 250–263.

Yilmaz, İ. 1975. *Alaçam Dağları granitlerinin petrojenetik etüdü.* Cumhuriyetin 50. Yılı kongresi tebliğleri, 457–473. Q8

Yilmaz, O. 1975. Etude pétrographique et staratigraphique de la région de Cacas (Massif de Bitlis, Turquie). *Bulletin of the Geological Society of Turkey*, **18**, 33–40. Q9

Yilmaz, Y. 1978. *Gevas (Van) dolayında Bitlis Masifi/Ofiyolit iliskisi. Türkiye*. **4**. Petrol Kongresi Bildiriler Kitabı, 83–93.

Yilmaz, Y. 1993. New evidence and model on the evolution of the southeast Anatolian orogen.

Bulletin of the Geological Society of America, **105**, 252–271.

Yilmaz, E. & Duran, O. 1997. Güneydogu Anadolu Bölgesi otokton ve allokton birimler stratigrafi adlama kılavuzu ‘Lexicon’. *Türkiye Petrolleri A.O. Arastırma Merkezi grubu Baskanlıgı, Egitim Yayınları*, **31**.

Yilmaz, O., Michel, R., Valette, Y. & Bonhomme, M. G. 1981. Réinterpétation des données isotopiques Rb-Sr obtenues sur les métamorphites de la partie méridionale du massif de Bitlis (Turquie). *Sciences Géologiques Bulletin, Strasbourg*, **34**, 59–73.

York, D. 1969. Least square fitting of a straight line with correlated errors. *Earth and Planetary science Letter*, **5**, 320–324.

Zor, E., Sandvol, E., Gurbuz, C., Turkelli, N., Seber, D. & Barazangi, M. 2003. The crustal structure of the East Anatolian plateau (Turkey) from receiver functions. *Geophysical Research Letters*, **30**. **Q6**